Role of a novel C-terminal motif in Pannexin 1 trafficking and oligomerization

by

Anna Epp
B.Sc., University of British Columbia Okanagan, 2015

A Thesis Submitted in Partial Fulfillment
of the Requirements for the Degree of

MASTER OF SCIENCE

in the Division of Medical Sciences

Supervisory Committee

Role of a novel C-terminal motif in Pannexin 1 trafficking and oligomerization

by

Anna Epp
B.Sc., University of British Columbia Okanagan, 2015

Supervisory Committee

Dr. Leigh Anne Swayne (Division of Medical Science)
Supervisor

Dr. Craig Brown (Division of Medical Sciences)
Departmental Member

Dr. Chris Nelson (Department of Biochemistry & Microbiology)
Outside Member

Abstract

Pannexin 1 (Panx1) is a metabolite channel enriched in the brain and known to localize to the cell surface, where it is involved in a variety of neuronal processes including cell proliferation and differentiation. The mechanisms through which Panx1 is trafficked or stabilized at the surface, however, are not fully understood. The proximal Panx1 C-terminus (Panx1CT), upstream of a caspase-cleavage site has been demonstrated to be required for Panx1 cell-surface expression. We discovered a previously unreported putative leucine-rich repeat (LRR) motif within the proximal Panx1CT. I investigated the involvement of this putative LRR motif on Panx1 localization and oligomerization. Deletion of the putative LRR motif or uniquely the highly conserved segment of the putative LRR motif resulted in a significant loss of Panx1 cell surface expression. Finally, ectopic expression of Panx1-EGFP in HEK293T cells increased cell proliferation, which was not recapitulated by a Panx1 deletion mutant lacking the putative LRR motif. Overall the findings presented in this thesis provide new insights into the molecular determinants of Panx1 trafficking and oligomerization.

Table of Contents

List of Tables

List of Figures

List of Abbreviations

AMPA – α-amino-3-hydroxy-5-methyl-4-isoxazolepropionic acid

AMPAR – AMPA receptor

ATP – adenosine triphosphate

BME – β-mercaptoethanol

BS3 – bis(sulfosuccinimidyl)suberate

CHX – cycloheximide

CNS – central nervous system

COPII – coatomer protein II

DTT – dithiothreitol

EGFP – enhanced green fluorescent protein

EL – extracellular loop

EMMPRIN – extracellular matrix metalloproteinase inducer

ER – endoplasmic reticulum

GAPDH – glyceraldehyde 3-phosphate dehydrogenase

GFP – green fluorescent protein

Gly0 – core, unglycosylated species of Panx1

Gly1 – high mannose glycosylated species of Panx1

Gly2 – complex N-linked glycosylated species of Panx1

GST – glutathione S-transferase

GT – glyceryl tripalmitate

HBSS – Hank's Balanced Salt Solution

HCS – highly conserved segment

HEK293T – human embryonic kidney 293T cells

LAP – LRR and PDZ

LRR – leucine-rich repeat

LRRC – leucine-rich repeat-containing protein

N2a – Neuro2a

PBS – phosphate buffered saline

Panx1 – Pannexin 1

Panx1CT – Pannexin 1 C-terminus

Panx2 – Pannexin 2

Panx3 – Pannexin 3

PDL – poly-D-lysine

PVDF – polyvinyldene fluoride

PDZ – PSD-95/Discs-large-ZO1

PEI – polyethylenamine

PFA – paraformaldehyde

PTM – post-translational modification

SDS – sodium dodecyl sulfate

SULF – 3- sulfogalactosylceramide

TARP – transmembrane AMPAR regulatory protein

TM – transmembrane

VRAC – volume-regulated anion channel

VS – variable segment

WGA – wheat germ agglutinin

Acknowledgments

There are so many people to whom I owe thanks for their support during the completion of my M.Sc. thesis work. First and foremost, I would like to thank my supervisor, Dr. Leigh Anne Swayne. In my time in her lab, she was always available and interested in aiding with my project. Through her mentorship I have gained invaluable skills in scientific method and rigor, concise communication, and the ability to tell a story. I thank her for her patience and support throughout my time in her lab, as well as for holding me to a high standard and for her passion for science. I would also like to thank my committee members, Dr. Chris Nelson and Dr. Craig Brown, who provided excellent perspectives and guidance throughout the duration of my project. Their feedback and encouragement over the years has been indispensable. Thank you to Dr. Dale Laird and Dr. Silva Penuela who provided the Panx1-EGFP construct used in this project.

I owe deep thanks to the numerous members of the Swayne Lab, both past and present. Dr. Andrew Boyce performed many of the membrane lipid strip assays in this study, trained me on several lab techniques, and provided kind and insightful feedback during preparation of the manuscript submitted during this study. I thank Dr. Leigh Wicki-Stordeur for creating two of the plasmid constructs used in this work and for her detailed review and opinions on the manuscript. I owe thanks to Dr. Juan Sanchez-Arias for the confocal imaging he performed for my project and for the stimulating conversations around Pannexin 1 activity and neuro/health science! Sarah Ebert aided me in countless (get it?) hours of cell counting; I thank her for her diligence, stringency, and patience during those assays as well as her cheerful and curious ways in the lab – they have been a true delight. I thank Dr. Olga Shevstova, Dr. Xiaoxue Xu, Dr. Mei Liu, Nicole York, Lena Chen, Maria Weaver, Megan Karpenko, Naomi Fuglem, Michelle Kim, and Nina Radisavljevic; each of these individuals were a joy to work with and contributed greatly to the

lab environment. Last but not least from the lab, I owe tremendous thanks to Catherine Choi. I thank her for her patience and opinions during times of lengthy troubleshooting, for her reliability and diligence in the lab, for our coffee break conversations (scientific and otherwise), and for her unwavering friendship – it has been irreplaceable to me in completing this degree.

I owe incredible thanks to my family and friends for their persistent support and understanding in busy periods and for enriching my life so deeply. I'd like to thank both my parents for teaching me the value of hard work and for supporting me in any pursuit. I feel honoured to have known my Dad and know he would be proud of me, and my Mom is truly an inspiration in my life.

Finally, I must thank my fiancé Michael McGregor, whose friendship and support went above and beyond over the last couple years, and has truly meant the world to me.

1. Introduction

1.1 Thesis overview

Pannexin 1 (Panx1) is a recently (Panchin et al. 2000) discovered large ion and metabolite channel that is ubiquitously expressed in vertebrates and particularly enriched in the brain (Baranova et al. 2004). This channel is best known for its ability to mediate the release of adenosine triphosphate (ATP) at the cell surface, where it is plays a role in both physiological and pathophysiological processes in a variety of cell types. In the perspective of the central nervous system, these include both neurogenesis, neuronal proliferation and differentiation (Wicki-Stordeur et al. 2012), as well as neuropathic pain (Bravo et al. 2014; Koyanagi et al. 2016; Zhang et al. 2015), seizure (Kim & Kang 2011; Santiago et al. 2011), and stroke (Bargiotas et al. 2011; Bargiotas et al. 2012). The mechanisms through which Panx1 is trafficked or stabilized at the surface to mediate its effects, however, are not fully understood.

In my thesis work I employ molecular biology tools to generate Panx1 deletion mutants, in conjunction with a variety of biochemical and imaging techniques to pinpoint a region in Panx1 that regulates its trafficking to the cell surface. Based on previous research and our own preliminary data, **I hypothesize there is a region within the proximal Panx1 C-terminus (Panx1CT) that is responsible for its cell surface localization.** I discover a previously unreported putative leucine-rich repeat motif (LRR; a motif that, when repeated, forms larger domains best known for its ability to mediate protein-protein interactions) in the Panx1CT that is necessary for cell surface localization. Finally, I investigate whether Panx1 increases proliferation in HEK293T cells (as our group had previously seen in Neuro-2a (N2a) cells; Wicki-Stordeur et al. 2012), and whether Panx1 lacking a full LRR sequence prompts the same or different effects.

This thesis is presented in a manuscript-based format. That is, Chapter 1 is a detailed review of

the current literature regarding Panx1 trafficking mechanisms. The central chapter, Chapter 2, is a manuscript submitted for publication, and contains the main data figures and methods. Chapter 3 provides a more in-depth discussion of the implications of this work to the field, suggestions for future work, and concluding remarks. Overall, this thesis provides important insights into the regulatory mechanisms of Panx1 trafficking.

1.2 Introduction to pannexins

1.2.1 Discovery

The pannexin family consists of 3 members of 4-transmembrane proteins: Panx1, Panx2, and Panx3, first discovered due to their homology to innexins, the invertebrate cousin of gap junction forming-connexins (Panchin et al. 2000). Because of their similarity to innexins, it was initially hypothesized that pannexins would function as gap junction-forming channels. Though pannexins have similar topology to innexins and connexins, they differ in a number of ways, including sequence homology and post-translational modifications. Thus, though there have been reports of gap junction-like activity of pannexins in ectopic expression systems (Bruzzone et al. 2003; Lai et al. 2007; Vanden Abeele et al. 2006; Ishikawa et al. 2011; Sahu et al. 2014), it is now accepted that these proteins do not form gap junctions (Huang et al. 2007; Sosinsky et al. 2011; Sahu et al. 2014), but rather act as single membrane spanning channels in the majority of cells it is expressed in.

1.2.2 Expression patterns

Pannexins exhibit different expression patterns across cells and tissues, as well as throughout development (reviewed in Boyce et al. 2018). Panx1 exhibits almost ubiquitous expression in mammalian cells (Baranova et al. 2004; Dvoriantchikova et al. 2006; Ivanov et al. 2006; Pelegrin &

Surprenant 2006; Penuela et al. 2007; Wang et al. 2009; Sridharan et al. 2010; Turmel et al. 2011; Lohman, Billaud, et al. 2012; Dolmatova et al. 2012; Riquelme et al. 2013), with particular enrichment in the central nervous system (CNS) at the level of both mRNA (Baranova et al. 2004) and protein (Penuela et al. 2007). Several studies have demonstrated that the levels of Panx1 dramatically decrease during CNS development, with peak expression occurring at embryonic day 18 in the mouse and postnatal day 1 in the rat, and drastically decreasing at postnatal day 15 and onwards (Vogt et al. 2005; Ray et al. 2005; Wicki-Stordeur & Swayne 2013). A decrease in Panx1 expression levels was also observed in N2a cells subjected to differentiation by retinoic acid (Wicki-Stordeur & Swayne 2013). Though original findings observing Panx1 mRNA in the CNS did not distinguish between neuronal and extra-neuronal Panx1 (Bruzzone et al. 2003; Baranova et al. 2004), recent studies have identified Panx1 in other cells of the CNS including astrocytes (Freitas-Andrade & Naus 2016; Garre et al. 2010; Koyanagi et al. 2016) and microglia (Burma et al. 2017). Panx2 expression was originally thought to be restricted to the CNS (Baranova et al. 2004), but subsequent studies suggest it may be expressed in other tissues (Bruzzone et al. 2003; Le Vasseur et al. 2014). Converse to Panx1, levels of Panx2 expression increase postnatally (Vogt et al. 2005; Swayne et al. 2010). Meanwhile, Panx3 is absent from the CNS, and is expressed in multiple other tissues such as skin, osteoblasts, lung, kidney, liver, thymus, and ear and tail cartilage (Penuela et al. 2007; Baranova et al. 2004; Bruzzone et al. 2003; Turmel et al. 2011; Langlois et al. 2014) and, like Panx2, demonstrates increased expression over development in rat skin (Langlois et al. 2014). Co-expression of pannexins has been observed in the CNS for Panx1 and Panx2 with both isotypes being expressed in the majority of neurons (Bruzzone et al. 2003; Vogt et al. 2005). There is some evidence that pannexins can function in a compensatory manner under unique circumstances, as suggested in a study using Panx1 and Panx2 single and double knockout models in the context of ischemic stroke (Bargiotas et al. 2011; Bargiotas et al. 2012). The temporal and spatial

variations in the expression of pannexins suggests they are involved in regulation of proliferation and differentiation in multiple cell types.

Of the 3 pannexins, Panx1 is by far the most studied, and is the focus of this study. As such, the rest of this chapter will turn its attention to Panx1, its structure and post-translational modifications, roles, activity, subcellular distribution, and known trafficking mechanisms.

1.3 Panx1

1.3.1 Structure and post-translational modifications (PTMs)

Panx1 is a 426 amino acid (42-48 kDa by Western blot), 4-pass transmembrane protein known to form hexameric channels capable of mediating the passage of molecules up to 1 kDa in size (reviewed in Boyce et al. 2018; Penuela et al. 2013). A crystal structure of Panx1 has not yet been obtained, though several studies utilizing *in silico* analyses and/or biochemistry have provided insight into the topology and secondary structure, as well as post-translational modifications (PTMs), of this protein. PTMs can have diverse impacts on Panx1 activity and trafficking in the cell (reviewed in Boyce et al. 2018). Figure 1.1 illustrates the structure of Panx1 and its various PTMs. Namely, Panx1 has been reported to be modified by N-linked glycosylation (Boassa et al. 2007; Penuela et al. 2007), phosphorylation (Weilinger et al. 2016; Iglesias et al. 2008; Lohman et al. 2015; Billaud et al. 2011), S-nitrosylation (Lohman, Weaver, et al. 2012; Penuela et al. 2014), and proteolytic cleavage (Chekeni et al. 2010; Sandilos et al. 2012).

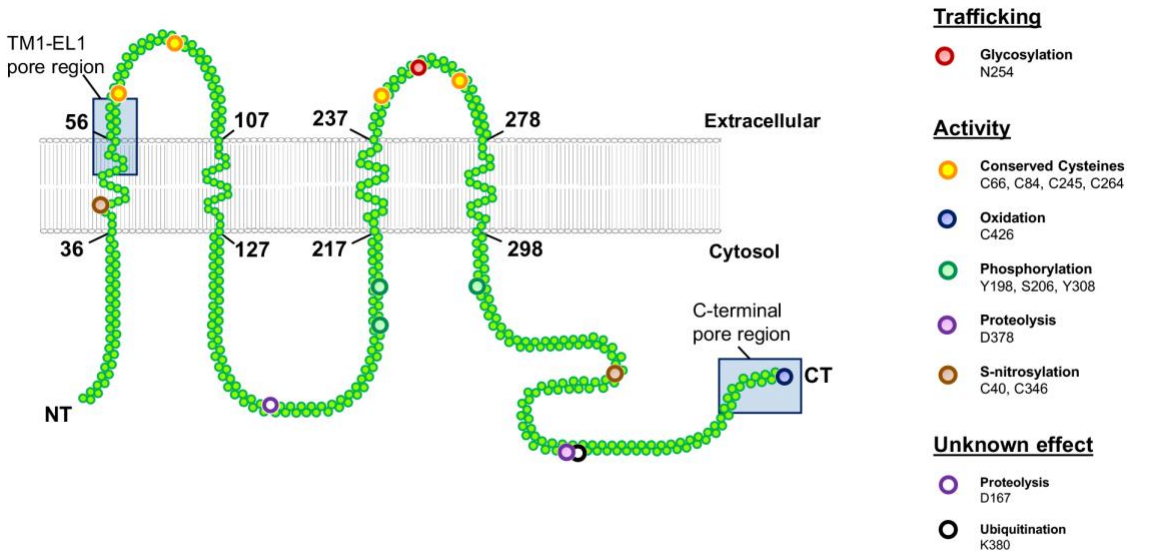

Figure 1.1. Panx1 structure and post-translational modifications (PTMs).

Amino acids are depicted in green circles and PTMs are enlarged circles. Numbered residues adjacent to the membrane indicate the first and last amino acid of each transmembrane (TM) domain, as per (Penuela et al. 2009). PTMs are classified according to whether they modify Panx1 trafficking, activity, or have unknown effects on channel behaviour (empty circle). Panx1 pore-lining residues from (Wang & Dahl 2010) are highlighted by the blue boxes. This figure was modified from (Boyce et al. 2018).

1.3.2 Roles and activity

Panx1 is best known for its ability to mediate the release of ATP. Though ATP was originally thought to function solely as a source of energy (reviewed in Khakh & Burnstock 2009), it is a molecule of diverse influences, including signaling between cells, often mediating its effects by acting on autocrine or paracrine purinergic receptors (reviewed in Dubyak & El-Moatassim 1993; Burnstock et al. 2011; Abbracchio et al. 2009; Burnstock 2016).

Additionally, Panx1 interacts with a variety of other receptors, including NMDA receptors

(Weilinger et al. 2016; Weilinger et al. 2012), P2X and P2Y purinergic receptors (Ohbuchi et al. 2011; Iglesias et al. 2008; Kim & Kang 2011; Draganov et al. 2015; Gulbransen et al. 2012; Silviu Locovei et al. 2006), TNF-α receptors (Lohman et al. 2015), and α-adrenergic receptors (Billaud et al. 2011; Billaud et al. 2015). Similarly, Panx1 is implicated in a variety of physiological and pathophysiological functions in a diversity of cell types (reviewed in Lohman & Isakson 2014), including activation of the cellular inflammasome (Crespo Yanguas et al. 2017), regulation of vascular tone (Lohman et al. 2015), recruitment of phagocytic cells towards dying cells (Chekeni et al. 2010), cancer progression (Penuela et al. 2012; Furlow et al. 2015), cell death (Weilinger et al. 2012; Gulbransen et al. 2012; reviewed in Swayne & Bennett 2016; Sanchez-Arias et al. 2016), propagation of Ca^{2+} waves (Silviu Locovei et al. 2006), neuronal development (Wicki-Stordeur et al. 2012; Wicki-Stordeur & Swayne 2013; Wicki-Stordeur et al. 2016), and modulation of CNS synaptic activity (Prochnow et al. 2009; Ardiles et al. 2014; Weilinger et al. 2016; Vroman et al. 2014).

Activation of Panx1 occurs through a variety of stimuli, including: mechanical stretch (Bao et al. 2004; S Locovei et al. 2006; Qiu et al. 2011; Seminario-Vidal et al. 2011), GPCR signaling (Billaud et al. 2011; Billaud et al. 2015), increased intracellular Ca^{2+} (Silviu Locovei et al. 2006), extracellular ATP via a positive feedback loop involving P2X7 receptors (P2X7Rs; Pelegrin & Surprenant 2006; Iglesias et al. 2008; reviewed in Baroja-Mazo et al. 2013), as well as increased extracellular potassium (Santiago et al. 2011), excitotoxic NMDAR activation (Weilinger et al. 2016; Thompson et al. 2008), oxygen and glucose deprivation/hypoxia (Thompson et al. 2006; Bargiotas et al. 2011), and irreversible cleavage of Panx1 at its C-terminal caspase cleavage site (Chekeni et al. 2010; Sandilos et al. 2012; Wang & Dahl 2018). Early work in oocytes suggested that Panx1 is also activated by voltage stimulation (Wang et al. 2014; Wang et al. 2018; W. Ma et al. 2012), however this is currently a matter of debate in the field that will require further elucidation (discussed in Chiu et al. 2018; Dahl 2018; Michalski et al. 2018).

Though the precise structure of the channel has not yet been determined, work from several groups suggests that that the pore of the hexameric channel is formed by the first transmembrane domain of each monomer, and that the Panx1 C-termini interact with the pore (see Fig. 1.1) (Wang et al. 2014; Sandilos et al. 2012; Chiu et al. 2017). This implies a "ball and chain" mechanism for activation of Panx1, in which the six C-termini of Panx1 hexamers are inserted in the pore of the channel until a stimulus is present; the conformation of Panx1 is then altered such that these C-termini are dislodged from pore. Further, the number of C-termini dislodged is related to the conductance of the channel (Chiu et al. 2017). The mechanisms of Panx1 conductance and permeabilities are complex and have been a matter of dispute over the years, particularly because different experimental conditions and species have resulted in different results (discussed in Chiu et al. 2018; Dahl 2018; Michalski et al. 2018). One of the current working models is that Panx1 can take on 2 or more different conformations that differ in permeabilities/conductance and functions (Dahl 2018).

Many of the downstream effects of Panx1 activation rely on its localization to the cell surface. Indeed endocytosis of Panx1 into intracellular compartments is one mechanism by which Panx1 can be regulated (Boyce et al. 2015; discussed in Jackson 2015). In the following sections, I discuss the current knowledge of Panx1 subcellular distribution and stability.

1.3.3 Subcellular distribution

The localization of both endogenously and exogenously expressed Panx1 at the cell surface has been widely confirmed in a multitude of cell types (Bhalla-Gehi et al. 2010; Cone et al. 2013; Lai et al. 2007; Vanden Abeele et al. 2006; Penuela et al. 2013; Boassa et al. 2007; Lohman et al. 2015; Beckmann et al. 2016; Penuela et al. 2007; Penuela et al. 2009). Distribution at the surface has been observed as highly mobile, diffuse and uniform, with some enrichment in microdomains (Bhalla-Gehi et al. 2010). In addition to cell surface expression, an intracellular

population of Panx1 is also commonly observed, and has been found to localize within early and recycling endosomes (Boyce et al. 2015), the endoplasmic reticulum (ER; Vanden Abeele et al. 2006), and lysosomes (Penuela et al. 2013; Boassa et al. 2007).

1.3.4 Regulation of stability and trafficking

Anterograde trafficking of Panx1 from the ER to the trans-Golgi proceeds through coatomer protein II (COPII)-coated vesicles (Bhalla-Gehi et al. 2010), and subsequently through the *trans*-Golgi network and finally to the cell surface. Interestingly, surface expression of Panx1 requires the post-translational modification, N-linked glycosylation (Penuela et al. 2007; Boassa et al. 2007; Penuela et al. 2009). Panx1 is glycosylated to 3 levels: a core, unglycosylated species (Gly0), a high-mannose species (Gly1) and a complexly glycosylated species (Gly2). Multiple labs employing glycosylation inhibitors and/or glycosylation-deficient mutants have reported that the glycosylation of Panx1 to the Gly2 level was required for Panx1 cell surface localization (Penuela et al. 2007; Boassa et al. 2007; Penuela et al. 2009), though a small population of the mutants were still capable of reaching the cell surface. Whether or not this loss of surface expression of unglycosylated Panx1 is due to a change in trafficking mechanisms or a loss of stability (potentially through interactions with the extracellular matrix or neighbouring interacting partners) is uncertain.

Panx1 exhibits long-term stability and slow turnover in measurements of both total protein (with a half-life >8 h; Penuela et al. 2007) and of cell surface populations (Panx1 was present at the cell surface >32 h (Penuela et al. 2013) and >18 h (Boassa et al. 2007) post-synthesis). Degradation of Panx1 is mediated by the lysosome (Gehi et al. 2011).

The mechanisms of retrograde trafficking of Panx1 have been elusive. Canonical mechanisms of

endocytosis, namely clathrin- or caveolin-dependent mechanisms, were ruled out based on studies utilizing specific disruptors of endocytic machinery (Gehi et al. 2011; Boyce et al. 2015). Panx1 endocytosis is dynamin-independent, further suggesting non-canonical mechanisms of endocytosis (Gehi et al. 2011; Boyce et al. 2015). Work from the Swayne lab demonstrated that Panx1 internalization is induced by ATP in a time- and dose-dependent manner, and is cholesterol-dependent (Boyce et al. 2015). This internalization requires activation of a purinergic receptor, P2X7R, and involves a direct interaction between the first extracellular loop of Panx1 and P2X7R (Boyce & Swayne 2017). P2X7Rs are inhibited by cholesterol and interact with lipid microdomains or lipid rafts (Robinson et al. 2014) which are regions in the cell membrane that are enriched in cholesterol, sphingolipids, and saturated phospholipids and implicated in trafficking of molecules to the cell membrane (reviewed in Bou Khalil et al. 2010). Additionally, Panx1 directly interacts with caveolin-1, a common constituent of some lipid rafts, though this interaction is not involved in ATP-stimulated Panx1 endocytosis (DeLalio et al. 2018). This suggests that Panx1 may interact with lipid microdomains, which could contribute to regulation of Panx1 membrane localization and stabilization.

The role of the Panx1CT in trafficking of Panx1 to the cell surface is of particular interest to this study. Previous work implicates the C-terminus in several capacities. First, the C-terminus is the most divergent region amongst the pannexin family – which have varied subcellular distributions (reviewed in Penuela et al. 2013). Panx1 and Panx3 possess C-termini of similar sequence homology and length and both traffic to the cell surface. In contrast, Panx2 has a larger C-terminus and localizes to intracellular compartments (Penuela et al. 2009). Further, direct interactions with the Panx1CT and actin have been confirmed, and disruption of actin polymerization resulted in an accumulation of intracellular Panx1-GFP (Bhalla-Gehi et al. 2010).

Several studies using deletion mutants further highlight the proximal Panx1CT as important for

cell surface localization (Gehi et al. 2011; Wicki-Stordeur et al. 2013; Dourado et al. 2014; Wang & Dahl 2018). Immunocytochemistry data in rat mammory cells and cell surface biotinylation data in HEK293T cells revealed a loss of surface localization of a Panx1 deletion mutant which entirely lacked its C-terminus (Panx1Δ307-RFP; Gehi et al. 2011). Additionally, immunocytochemistry and cell surface biotinylation data from the Swayne lab showed that the Panx1CT of a Panx2^{Panx1CT} chimeric protein was unable to redirect intracellular Panx2 to the cell surface in N2a cells (Wicki-Stordeur et al. 2013). Taken together these data suggest that, though the C-terminus was necessary, it was not sufficient to mediate cell surface localization; though one cannot rule out the possibility of other factors at play in the case of the chimer, such as regions of Panx2, or lack of complex Panx2 glycosylation, sequestering the mutant intracellularly or preventing its surface stabilization. Other Panx1CT partial deletion mutants have been studied, including a construct coding for mouse Panx1 truncated after its caspase cleavage site (Δ379; Dourado et al. 2014). The Δ379 mutant was still able to traffic to the cell surface and was capable of mediating current. Likewise, Wang et al. (Wang & Dahl 2018) recently observed the channel properties of a similar mutant, mouse Panx1Δ378, in oocytes using electrophysiology. The ability of both groups to detect current with these constructs suggests that Panx1 lacking its distal C-terminus is capable of reaching the cell surface. Further, these data suggest that a region in the proximal C-terminus (upstream from aa 378) is important for trafficking of Panx1 to the cell surface.

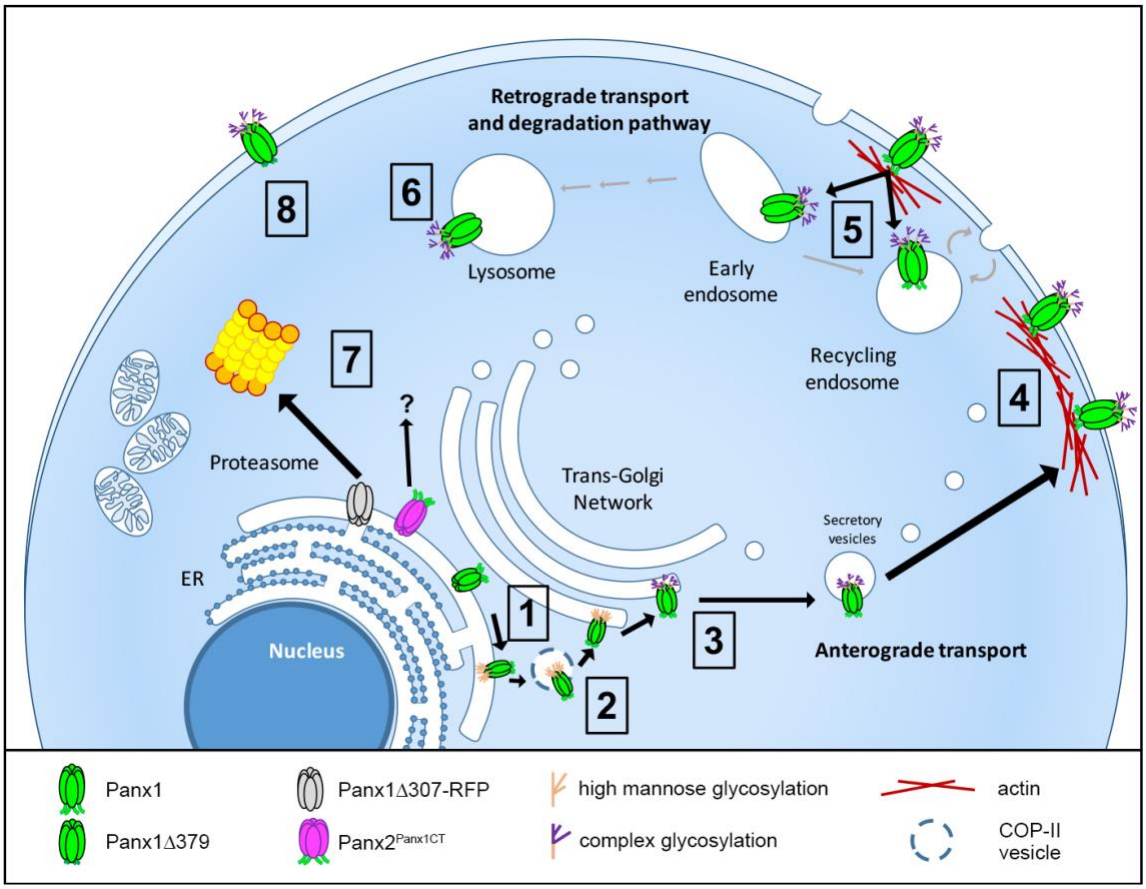

Figure 1.2. Panx1 trafficking.

(1) Anterograde trafficking of Panx1 begins in the ER, where it is glycosylated to a high mannose species. (2) Transport to the Golgi Apparatus is mediated by COP-II vesicles. (3) Panx1 is further glycosylated to a complex degree in the Golgi, then trafficked to the cell surface. (4) The Panx1CT interacts with actin. (5) Internalization of Panx1 is induced by ATP, is cholesterol-dependent, and results in Panx1 trafficking to endosomes. (6) Panx1 is degraded in the lysosome. (7) A Panx1 deletion mutant that lacks its C-terminus is degraded by the proteasome, while the $Panx2^{Panx1CT}$ chimer has diffuse intracellular localization. (8) A deletion mutant lacking the region past the caspase cleavage site still traffics to the cell surface. These data suggest that the proximal Panx1CT is required for cell surface localization.

1.4 Leucine-rich repeats (LRRs)

LRR motifs are 20-30 residues long and were first observed in 1985 in α_2-glycoprotein (Takahashi et al. 1985). A very high leucine content and unique repetition led to the hypothesis of an organized motif. Without a crystal structure, the secondary structure of this novel motif was only a prediction, based on Chou-Fasman rules (Chou & Fasman 1978). The first crystal structure of an LRR was obtained in 1993 – on ribonuclease inhibitor extracted from pig liver (Kobe & Deisenhofer 1993). From this structure and future work on this and other LRR motif-containing proteins, it was discovered that a single LRR motif is composed of a highly conserved segment (HCS) which normally forms a β-strand, followed by a variable segment (VS), which usually forms an α-helix (reviewed in Ng et al. 2011; Bella et al. 2008). The HCS typically consists of a 12-residue sequence LxxLxLxxCxxL or an 11-residue sequence LxxLxLxxNxL, where L is Leu, Ile, Val, or Phe (but can be any hydrophobic amino acid); N is Asn, Thr, Ser, or Cys; and C is Cys, Ser, or Asn (Ng et al. 2011; Bella et al. 2008; Kajava 1998; Kobe & Kajava 2001). Additionally, the first and last L can be replaced by a relatively hydrophilic residue (Matsushima et al. 2007). There are at least 8 different types of LRR motifs (consisting of an HCS and VS), organized according to consensus sequence similarity: typical (the most common LRR motif), RI (ribonuclease inhibitor)-like, CC (cysteine-containing), GALA (a subclass of CC type LRRs), PS (plant-specific), SDS22-like, bacterial, and TpLRR (named as they are found in *Treponema pallidum*)(Matsushima et al. 2010). Each type of LRR motif has its own overall (HCS and VS) consensus sequence (reviewed in Matsushima et al. 2010; Kobe & Kajava 2001; Kajava 1998).

Multiple (between 2-60) LRR motifs usually go on to form an LRR domain, which frequently consist of a canonical horseshoe shape (Fig. 1.3) and mediate interactions with a variety of ligands (reviewed in Bella et al. 2008; Ng et al. 2011). Overall these domains are involved in a variety of processes, including cell adhesion and signaling (Kresse & Schnherr 2001; Matilla & Radrizzani 2005;

Hohenester et al. 2006), extracellular matrix assembly (Hocking et al. 1998), platelet aggregation (Andrews & Berndt 2004), neuronal development (Chen et al. 2006; Ko & Kim 2007; de Wit et al. 2011), RNA processing (Price et al. 1998; Liker et al. 2000), and immune response (Martinon & Tschopp 2005; Rogozin et al. 2007; West et al. 2006; Pancer & Cooper 2006). While the convex side of the horseshoe is commonly composed of the α-helical (or other secondary structured) VS, the concave side is usually composed of the β-sheets of the HCS, and frequently functions as the ligand-binding site. However, the sequence and structure of each repeat and overall domain can vary greatly between proteins. LRR domains are considered to be promiscuous in nature, having the potential to interact with a variety of partners, perhaps simultaneously (Bella et al. 2008). The general lack of rigidity in the consensus sequence of LRR motifs makes them difficult to identify.

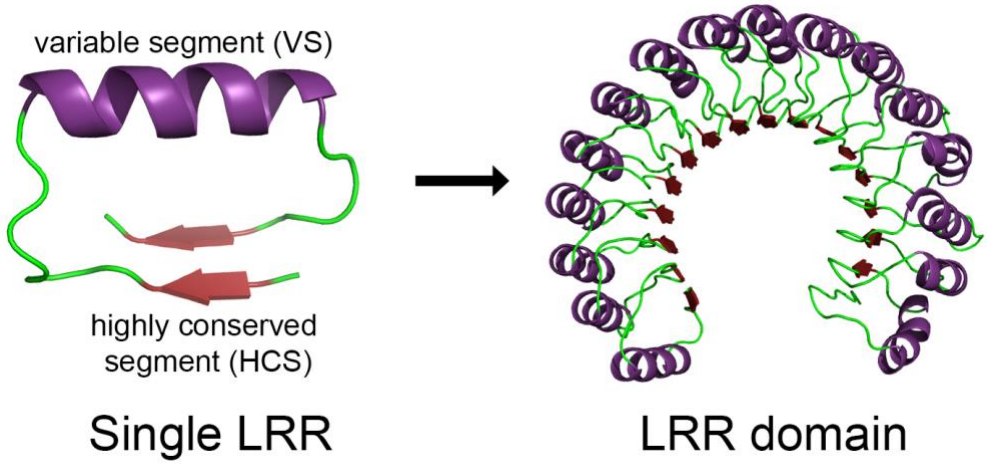

Figure 1.3. Example of a leucine-rich repeat (LRR) and LRR domain.

An example image of the structure of a single LRR and an LRR domain (generated using PyMOL; from ribonuclease inhibitor, PDB: 2bnh).

1.4.1 Homology of Panx1 with other LRR-containing proteins

Little is known regarding the evolutionary origins of LRR domains. It is possible that the domain originated from a single common ancestor (Andrade et al. 2000). However, as there is high conservation within each individual class of LRR motif, the possibility that different classes were a result of separate origins has also been proposed (Kajava 1998).

Interestingly, Panx1 was found to share ancestry, sequence homology (from the N-terminus to the fourth transmembrane domain), and similarities in localization as an LRR-containing protein, LRRC8A (Abascal & Zardoya 2012). LRRC8A, also known as SWELL1, is an obligatory subunit of VRAC (volume-regulated anion channels) and important for regulation of cell volume. Like Panx1, it mediates the release of ATP and is involved in cell proliferation (reviewed in Pedersen et al. 2016). The LRR domain in LRRC8A has been confirmed by X-ray crystallography, and also resides in the intracellular C-terminus of the channel. It should be noted that while no homology was detected between the Panx1CT and the LRRC8A C-terminus in the study identifying their homology (Abascal & Zardoya 2012), this was not specifically investigated and might have been overlooked due to relatively stronger homologies within other parts of the proteins.

1.4.2 Role of LRR domains in protein trafficking and membrane localization

The ability of LRR domains to mediate protein trafficking stems from their nature as mediators of protein-protein and protein-lipid interactions (reviewed in Bella et al. 2008; Ng et al. 2011). Interactions such as these can be important for proper protein localization. For example, AMPA receptors (AMPARs) interact with transmembrane AMPAR regulatory protein (TARP) to facilitate its export from the ER; disruption of this interaction results in mislocalization of AMPARs (reviewed in Jacobi & von Engelhardt 2018). Similarly, disruption or changes to an LRR domain that alter intermolecular interactions could change the localization

of that LRR-containing protein. For instance, deletion of an LRR domain in members of the LRR and PDZ (LAP; PDZ, PSD-95/Discs-large-ZO1) family of proteins resulted in a loss of proper localization to the basolateral membrane of epithelial cells (Legouis et al. 2003).

1.5 Summary and hypothesis

Previous work suggested that the proximal Panx1CT is required for cell surface localization of Panx1 (Gehi et al. 2011; Wicki-Stordeur et al. 2013; Dourado et al. 2014; Wang & Dahl 2018). I discovered a putative, previously unreported LRR motif and several LRR HCS sequences in the proximal Panx1CT, which led me to my main research questions (Fig. 1.4). Based on these findings, I hypothesized that:

1) *A region within the proximal Panx1 C-terminus (Panx1CT) is responsible for cell surface localization of Panx1.*
2) *The putative LRR(s) in the proximal Panx1CT regulate Panx1 trafficking.*

1.5.1 Aim 1: Identify which amino acids in the Panx1CT are responsible for cell surface localization of Panx1.

The proximal Panx1CT is required for cell surface localization of Panx1 (Gehi et al. 2011; Wicki-Stordeur et al. 2013; Dourado et al. 2014; Wang & Dahl 2018). In Aim 1 of this thesis, I employ cell surface biotinylation and confocal imaging tools to confirm the impact deletion of the entire Panx1CT (Panx1Δ299-EGFP) or of the distal Panx1CT (Panx1Δ379-EGFP, mimicking the caspase cleaved Panx1) on cell surface localization of EGFP-tagged Panx1 in HEK293T cells. HEK293T are reported to lack Panx1 expression (however, Sanchez-Pupo et al. 2018 did recently identify a population of endogenous Panx1 in these cells). Further, I investigate the glycosylation state and oligomerization properties of these same Panx1 deletion mutants. Specifically, this aim addresses several key research

questions:

- *Is the proximal Panx1CT required for cell surface localization of Panx1?*
- *Is the distal Panx1CT required for oligomerization of Panx1 into hexamers?*

1.5.2 Aim 2: Identify the role of the LRR motif in Panx1 cell surface localization.

I discovered a putative LRR motif and several LRR HCS consensus sequences that perfectly match the LRR motif consensus sequence criteria. Multiple LRR motifs form LRR domains that can influence protein localization and interactions. In Aim 2 of this thesis, I employ cell surface biotinylation, confocal imaging, deglycosylation assays, and crosslinking assays to address how deletion of the putative LRR motif, HCS, or VS from the Panx1CT influences cell surface localization, glycosylation, or oligomerization states of EGFP-tagged Panx1 in HEK293T cells. This aim addresses the following key research question:

- *Is the putative LRR motif required for cell surface localization?*
- *Is the HCS or VS of the putative LRR motif required for cell surface localization?*

1.5.3 Aim 3: Identify how deletion of the LRR motif influences the ability of Panx1 to increase cell proliferation.

Previous work by our lab demonstrated that Panx1 increases N2a cell proliferation (Wicki-Stordeur et al. 2012). In Aim 3, I employ Trypan blue proliferation assays and MTT assays to investigate whether EGFP-tagged Panx1 increases HEK293T cell proliferation, and whether Panx1 lacking a full LRR motif exhibits the same or different effects. This aim addresses the research questions:

- *Does Panx1 increase HEK293T cell proliferation?*
- *Is the putative LRR motif required for increases in cell proliferation?*

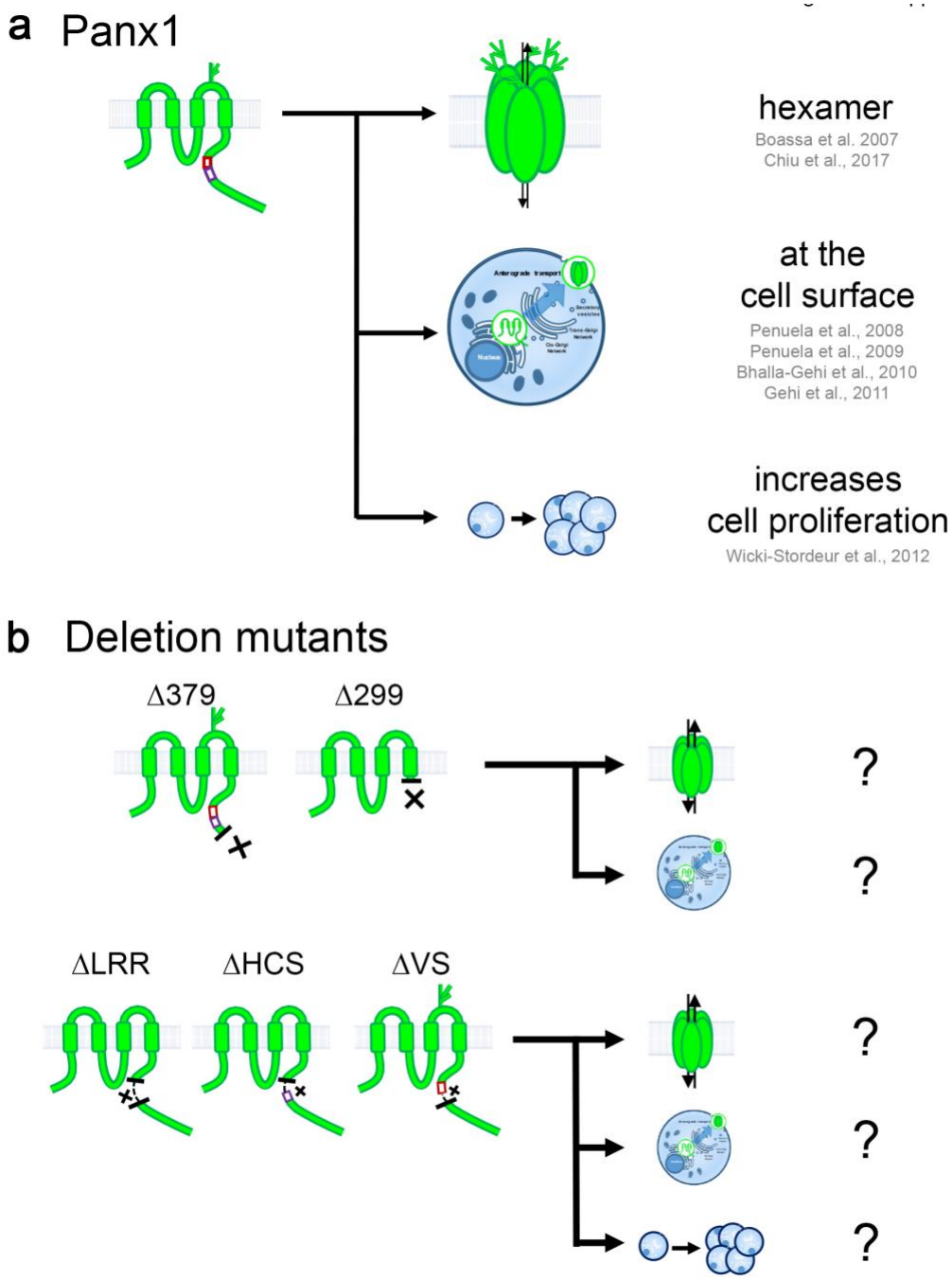

Figure 1.4. Research questions.

(a) Previous research demonstrated that Panx1 forms hexamers that traffic to the cell surface, and result in an increase in cell proliferation. The mechanisms of how Panx1 is trafficked to the cell surface, however, are not fully understood, but studies have implicated the proximal Panx1CT as

a requirement. The aim of my thesis is to address whether specific amino acids in the proximal Panx1 C-terminus are responsible for its trafficking to the cell surface, focusing in on the novel and putative LRR motif that I discovered in this region. To study this, I use (b) EGFP-tagged deletion mutants in conjunction with several biochemical and imaging techniques to observe their localization, glycosylation (a molecular signature of Panx1 cell surface localization), and oligomerization. I further investigate if Panx1 increases proliferation in HEK293T cells as it did in N2a cells, and whether Panx1 lacking a full LRR motif has the same or different effect.

2. A novel motif in the proximal C-terminus of Pannexin 1 regulates cell surface localization

(2019, *In Review*)

Anna Epp[1], Andrew KJ Boyce[1], Sarah Ebert[1], Leigh Wicki-Stordeur[1], Juan Sanchez-Arias[1], Leigh Anne Swayne[1,*]

[1]Division of Medical Sciences and Island Medical Program, University of Victoria, Victoria, V8P 5C2, Canada

*Corresponding author at: Division of Medical Sciences, 3800 Finnerty Rd, Victoria, BC, Canada. Email address: lswayne@uvic.ca (L.A. Swayne); twitter: @dr_swayne

Author Contributions:

A.E., A.K.J.B., and L.A.S. designed the research. A.E performed the majority of the experiments. S.E. aided in cell proliferation assays. L.W.S. created the Panx1Δ299-EGFP and Panx1Δ379-EGFP plasmid. J.S.A. aided in confocal imaging. A.E. and L.A.S. wrote the manuscript.

Acknowledgments

This work received operating grant support to L.A.S. from the Natural Sciences and Engineering Research Council (NSERC) [RGPIN-2017-03889]. The Leica SP8 confocal microscope was purchased with funds from the Canada Foundation for Innovation (CFI) [grant number 29462],

and the BC Knowledge Development Fund (BCKDF) [grant number 804754] and the University of Victoria awarded to L.A.S. L.A.S. also received a Scholar Award from the Michael Smith Foundation for Health Research (MSFHR) and British Columbia Schizophrenia Society Foundation [grant number 5900]. A.E. was supported by UVic Graduate Awards. A.K.J.B. was supported by student scholarships from NSERC [PGSD 459931-2014] and the University of Victoria (President's Research Scholarship, and Dr. Julius F. Schleicher Memorial Scholarship). L.W.S. was supported by Vanier Canada Graduate Scholarships (NSERC). J.S.A. was supported by a University of Victoria Fellowship Graduate Award. We would also like to thank Drs. Laird and Penuela for their generous gift of the mouse Panx1-EGFP plasmid.

2.1 Abstract

Pannexin 1 (Panx1) is an ion and metabolite channel involved in a variety of cell behaviours including cell proliferation and differentiation. Previous work suggests that a region within the proximal Panx1 C-terminus (Panx1CT) regulates its trafficking to the cell surface. Here we report the discovery of a putative leucine-rich repeat (LRR) motif in the proximal Panx1CT necessary for Panx1 cell surface expression in HEK293T cells. Deletion of the highly conserved segment of the LRR motif results in a significant loss of Panx1 cell surface distribution. Further, deletion of the highly conserved segment of the LRR precludes the enhancing effect of Panx1 on HEK293T cell proliferation. Overall these findings provide new insights into the molecular mechanisms underlying C-terminal regulation of Panx1 trafficking.

2.2 Introduction

Pannexin 1 (Panx1) is a four-transmembrane domain protein that oligomerizes in hexamers to form ion and metabolite channels, and is detected at the cell surface and intracellular membranes (reviewed in Boyce et al. 2018). The factors regulating Panx1 trafficking and cell surface localization have been the focus of intense study, identifying glycosylation state (Penuela et al. 2007; Boassa et al. 2007; Penuela et al. 2009) and the intracellular C-terminus (Bhalla-Gehi et al. 2010; Gehi et al. 2011; Wicki-Stordeur et al. 2013) as important contributors. The cumulative data of several studies suggests that the Panx1 C-terminus (Panx1CT) is required, but not sufficient for cell surface localization. Panx1CT deletion in rat mammory cells resulted in a loss of Panx1 cell surface localization (Gehi et al. 2011). Furthermore, substitution of the Panx2 C-terminus with that of Panx1 was not sufficient to direct the usually intracellular Panx2 to the cell surface in Neuro-2a (N2a) cells (Wicki-Stordeur et al. 2013). In addition, distal Panx1CT deletion mutants retain cell surface expression and/or function that is dependent on surface localization (Dourado et al. 2014; Wang & Dahl 2018). Together these previous studies suggest a region in the proximal C-terminus is important for trafficking of Panx1 to the cell surface.

In the present study, we seek to expand our understanding of Panx1CT regulation of cell surface expression. We created EGFP-tagged Panx1CT deletion mutants and examined their surface expression along with two other key properties that provide additional insight: glycosylation and oligomerization state. Panx1 exhibits 3 main glycosylation states: Gly0 (unglycosylated), Gly1 (high-mannose species), and Gly2 (complex glycosylation) (Penuela et al. 2007; Boassa et al. 2007; Penuela et al. 2009). The complex glycosylation species of wild type Panx1 is more frequently associated with cell surface expression (Penuela et al. 2007; Boassa et al. 2007; Penuela et al. 2009), providing an important additional molecular signature

when assessing surface expression. In terms of oligomerization state, it is not yet known how Panx1 cell surface expression and hexamerization (Boassa et al. 2007; Chiu et al. 2017; Wang et al. 2014) are connected; it is entirely possible that Panx1 could reach the cell surface prior to oligomerization, which is important for its functional properties (Chiu et al. 2017). We therefore investigate the localization, glycosylation, and oligomerization profiles of EGFP-tagged Panx1CT deletion mutants in HEK293T cells, which lack appreciable endogenous Panx1 expression at the protein level (however see Sanchez-Pupo et al. 2018).

Our new data suggest that the proximal Panx1CT (residues R299-D378) is necessary for Panx1 cell surface localization. Within this region we identify the consensus sequence of a novel 21 amino-acid long leucine-rich repeat motif (LRR; S328-K348). Multiple LRR motifs are known to form LRR domains, which are solenoidal protein structures recognized for their ability to mediate interactions with a variety of ligands (reviewed in Bella et al. 2008), and thus have the potential to influence the localization or stabilization of a protein to specific regions throughout the cell. For example, in LRR and PDZ (LAP; PDZ, PSD-95/Discs-large-ZO1) proteins, the LRR domain is required for targeting to the basolateral membrane of epithelial cells (Legouis et al. 2003). In addition, we confirm that Panx1 expression increases cell proliferation in HEK293T cells (as it does in N2a cells; Wicki-Stordeur et al. 2012), and investigate the impact of deletion of the putative LRR motif. Overall, this study provides important new insights into the role of the Panx1CT in cell surface localization, identifying a putative LRR motif within the proximal C-terminus that is required for cell surface localization.

2.3 Results

2.3.1 A region in the proximal Panx1CT is required for cell surface localization

We first generated constructs with large deletions of the C-terminus (Fig. 2.1a): the entire C-terminus (Panx1Δ299-EGFP) and the region distal to a C-terminal caspase cleavage site (Panx1Δ379-EGFP). We used cell surface biotinylation and confocal imaging to determine the localization of Panx1-EGFP and these Panx1CT deletion mutants. There was no significant difference between surface levels of Panx1-EGFP and Panx1Δ379-EGFP, consistent with previous reports (Dourado et al. 2014). However, we detected substantially less Panx1Δ299-EGFP at the cell surface (Fig. 2.1b). Similarly, confocal imaging revealed co-distribution of Panx1-EGFP and Panx1Δ379-EGFP with the surface marker wheat-germ agglutinin (WGA) while Panx1Δ299-EGFP did not co-distribute with WGA (Fig. 2.1c). We also investigated the glycosylation state of these C-terminus deletion mutations using de-glycosylation enzymes that target immature (high-mannose) and mature (complex) glycosylation states. The glycosylation states of Panx1-EGFP and Panx1Δ379-EGFP were similar to one another (Fig. 2.1d). The Gly1 and Gly2 bands in Panx1-EGFP and Panx1Δ379-EGFP samples were sensitive to PNGase F treatment (Fig. 2.1d*i*), confirming complex N-linked glycosylation, which has been previously associated with cell surface expression (Penuela et al. 2007; Boassa et al. 2007; Penuela et al. 2009). However, only Gly0 and Gly1 forms were detected for Panx1Δ299-EGFP (Fig. 2.1d), which exhibited reduced expression levels (Supplementary Fig. S1), as previously reported (Gehi et al. 2011). Together these data confirm that the proximal C-terminus is required for cell surface localization of Panx1, as suggested by previous reports (Gehi et al. 2011; Dourado et al. 2014; Wang & Dahl 2018).

While the above data yielded no information about the ability of Panx1Δ379-EGFP to form oligomers, the functionality of Panx1Δ378 (Dourado et al. 2014; Wang & Dahl 2018)

suggests that it does. To directly determine the oligomerization state of Panx1Δ379-EGFP at the cell surface, we used a cell-impermeable crosslinker, BS^3, and compared oligomerization properties with full length Panx1-EGFP using Western blot (Fig. 2.2). Panx1-EGFP formed hexamers as previously reported (Boassa et al. 2007; Chiu et al. 2017; Wang et al. 2014). The Panx1Δ379-EGFP mutant formed oligomers that corresponded to those of Panx1-EGFP (relative to molecular weight; Fig. 2.2a*ii*,b). That is, there were no significant differences in relative abundance of hexameric, intermediate, or monomeric bands. It is important to note that under these conditions we are not able to discern whether monomeric bands originate from intracellular or cell surface pools. We did not detect high molecular weight species corresponding to intermediate oligomers or hexamers in the Panx1Δ299-EGFP samples, which was expected given its restricted cell surface localization that is requisite for exposure to BS^3 (Fig. 2.2a*iii*,b). We did not detect any higher molecular weight bands with longer exposures (data not shown). These results confirm that cell surface proteins formed oligomers in similar abundance, i.e. oligomerization profile was conserved with the deletion of the distal C-terminus. Overall, these results suggest that a region within the proximal Panx1CT is required for its trafficking to the cell surface and that the distal Panx1CT is dispensable for oligomerization of Panx1. We thus asked whether there are specific amino acids in the proximal Panx1CT that regulate Panx1 trafficking.

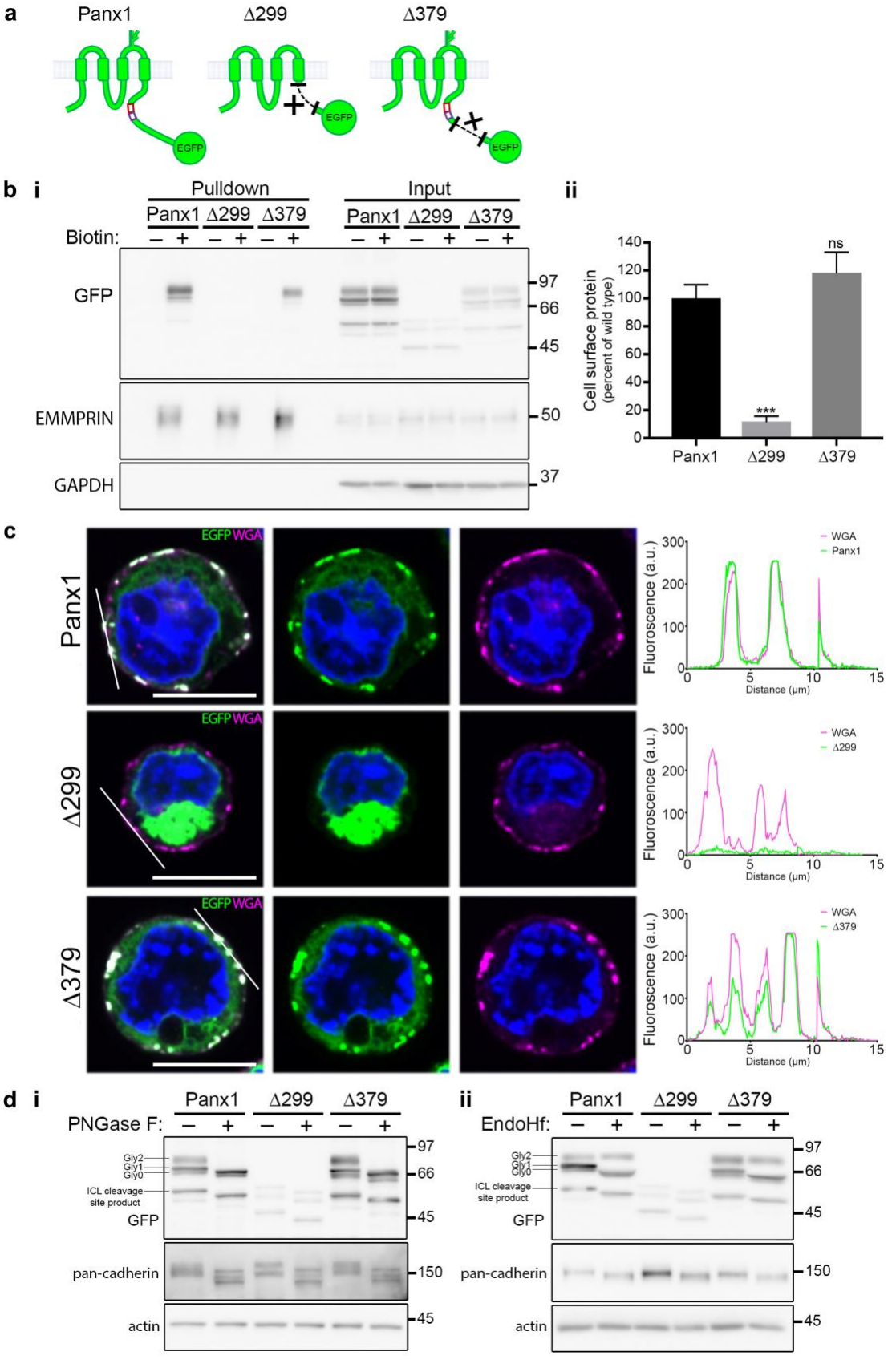
a
Panx1
Δ299
Δ379
EGFP
b i
Pulldown
Input
Panx1 Δ299 Δ379
Panx1 Δ299 Δ379
Biotin:
GFP
EMMPRIN
GAPDH
97
66
45
50
37
ii
Cell surface protein
(percent of wild type)
ns
***
Panx1
Δ299
Δ379
c
EGFP WGA
Panx1
Δ299
Δ379
Fluorescence (a.u.)
Distance (μm)
WGA
Panx1
Δ299
Δ379
d i
PNGase F:
ii
EndoHf:
Gly2
Gly1
Gly0
ICL cleavage site product
GFP
pan-cadherin
actin
150

Figure 2.1. The proximal Panx1CT is necessary for cell surface localization of Panx1-EGFP.

(a) Schematic of full length Panx1-EGFP and the Panx1Δ299-EGFP and Panx1Δ379-EGFP deletion mutants. (b) Cell surface biotinylation assays reveal that the proximal Panx1CT is required for cell surface localization in HEK293T cells. (*i*) Representative Western blot of pulldown (cell surface protein) and input. Anti-EMMPRIN was used as a positive control for biotin pulldown and as a loading control, and anti-GAPDH was used as a negative control against biotin internalization. (*ii*) Panx1Δ299-EGFP exhibited reduced cell surface levels compared to Panx1-EGFP, while surface levels of Panx1Δ379-EGFP were similar to those of Panx1-EGFP. Data are presented as mean ± SEM. One-way ANOVA with Dunnett's multiple comparisons test, $N = 3$, $\alpha = 0.05$, $F(2,6) = 62.39$, $^{**}p = 0.0002$, ns, nonsignificant. (c) Confocal images of HEK293T cells overexpressing Panx1-EGFP, Panx1Δ379-EGFP, or Panx1Δ299-EGFP (green). Hoechst was used as a nuclear counterstain (blue) and wheat-germ agglutinin (WGA) was used as a plasma membrane marker (magenta). Overlapping EGFP and WGA signals (white) and line scans along the cell membrane reveal cell surface localizaton of each protein. Panx1-EGFP and Panx1Δ379-EGFP co-distributed with WGA, while Panx1Δ299-EGFP did not. $N = 3$. Scale bars, 10 μm. (d) Deglycosylation assays using (*i*) PNGase F or (*ii*) EndoHf reveal Panx1-EGFP and Panx1Δ379-EGFP exhibited Gly0, Gly1, and Gly2 glycosylation species, while Panx1Δ299-EGFP exhibited only Gly0 and Gly1 forms. Anti-pan-cadherin and anti-β-actin were used as a positive and negative controls for deglycosylation, respectively.

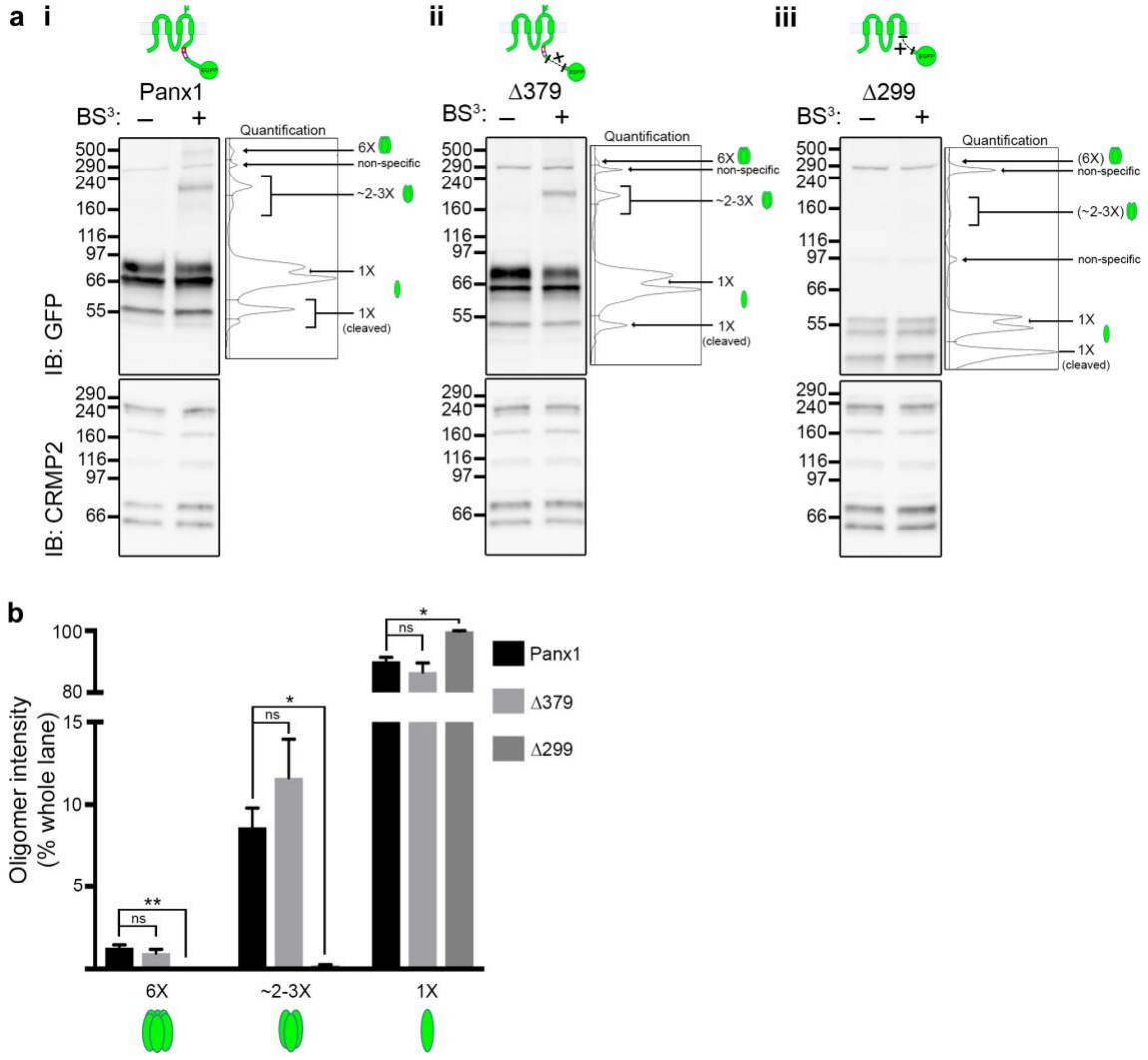

Figure 2.2. Surface oligomerization is preserved with deletion of the distal Panx1CT.

(a) Crosslinking assays reveal oligomerization profiles of C-terminal deletion mutants. Representative Western blots observing HEK293T cell lysates post-transfection with (*i*) Panx1-EGFP, (*ii*) Panx1Δ379-EGFP, or (*iii*) Panx1Δ299-EGFP, and after crosslinking with the cell-impermeable crosslinker, BS^3, to observe surface-localized oligomers (6X or ~2-3X). The plot of each quantification is included to shed light on the analytical process. An antibody for Crmp2, an intracellular protein known to form tetramers, was used as a negative control to ensure BS^3 had not entered the cell. Crmp2 oligomerization did not increase in the presence of BS^3, as expected.

(b) Each oligomeric band was quantified and expressed as a percentage of the entire GFP signal in each lane. Non-specific bands were excluded from the analysis. Mutants lacking the distal Panx1CT (Panx1Δ379-EGFP) had the same oligomerization profiles as full length Panx1-EGFP. Data are presented as mean ± SEM. One-way ANOVA with Dunnett's multiple comparisons test, $N = 3$, $\alpha = 0.05$; $F(2,6) = 17.59$, $^{**}p = 0.0023$ (6X); $F(2,6) = 15.73$, $^{*}p = 0.0127$ (3X); $F(2,6) = 13.84$, $^{*}p = 0.0169$ (1X); ns, nonsignificant.

2.3.2 A putative leucine-rich repeat motif in the proximal Panx1CT is required for cell surface localization

The ScanProsite tool (de Castro et al. 2006) was used to detect previously unidentified motifs within the mouse Panx1 amino acid sequence (NCBI accession number: NP_062355.2) that could contribute to Panx1 localization. The scan (using high-sensitivity settings) uncovered a previously unreported putative leucine-rich repeat (LRR) motif at residues S328-K348 (Fig. 2.3). Further examination revealed the putative LRR motif perfectly fit the criteria: single LRRs typically consist of a highly conserved segment (HCS) of 11-12 residues consisting of LxxLxLxxNxL or LxxLxLxxCxxL; where L is Leu, Ile, Val, or Phe (but can be replaced by any hydrophobic amino acid); N is Asn, Thr, Ser, or Cys; and C is Cys, Ser, or Asn; and where the first and last L can be replaced by relatively hydrophilic residues, followed by a variable segment (VS) (Kobe & Kajava 2001; Kajava 1998; Matsushima et al. 2007; Enkhbayar et al. 2004; Ng et al. 2011; Bella et al. 2008). As multiple (2 or more) LRR motifs are usually found in relatively close proximity in a protein sequence to form solenoidal LRR domains (Bella et al. 2008; Ng et al. 2011), we further inspected the amino acid sequence for adjacent LRR motifs within the Panx1CT. We discovered an additional 4 sequences consistent with the HCS consensus criteria and numbered each segment HCS1-HCS5 (Fig. 2.3). These sequences are conserved between

mouse, human, and rat Panx1CT. As these additional HCS sequences were not identified by ScanProsite, we were not able to identify prospective VS included within each corresponding LRR motif.

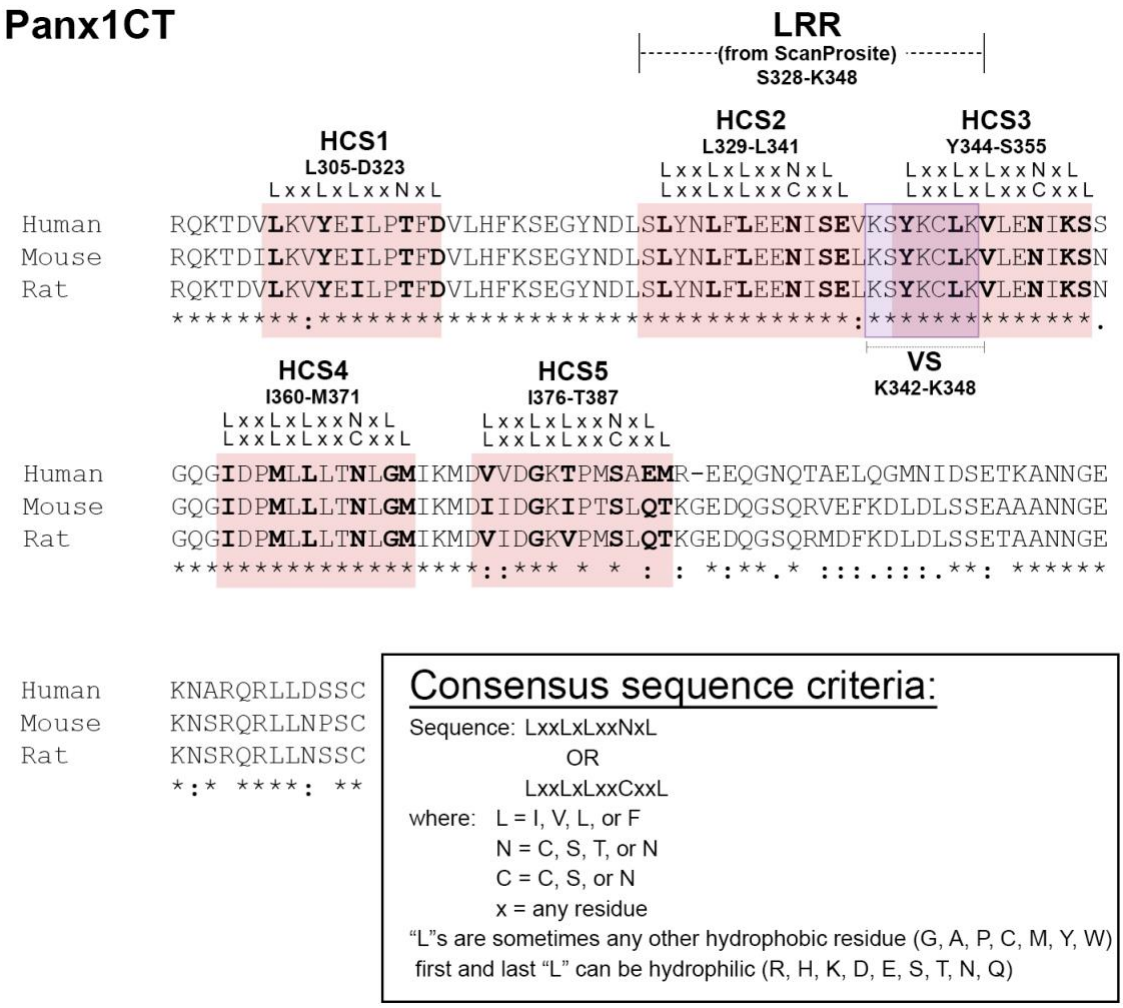

Figure 2.3. The Panx1CT amino acid sequence contains 5 LRR HCS consensus sequences. Sequence alignment of Panx1CT from human, mouse, and rat. Each of the identified HCS regions are indicated in red, and labeled with the corresponding consensus sequence. The VS proposed by ScanProsite is indicated in purple. The alignment was generated using CLUSTAL O

(1.2.3) with NCBI accession numbers: NP_056183.2 (human), NP_062355.2 (mouse), and NP_955239.1 (rat).

In light of the discovery of the putative LRR motif and the additional LRR HCS, together with previously reported shared ancestry and sequence conservation between Panx1 and LRRC8A, an LRR-containing protein (Abascal & Zardoya 2012), we investigated the hypothesis that these C-terminal putative LRR motifs play a role in Panx1 cell surface localization. We started with the putative LRR motif at S328-K348 identified by ScanProsite (containing an HCS and an identified VS). We generated a full S328-K348 LRR motif deletion mutant (Panx1ΔLRR-EGFP) as well as 2 partial LRR deletion mutants targeting separately the HCS at S328-L341 (Panx1ΔHCS-EGFP) and the VS at K342-K348 (Panx1ΔVS-EGFP; Fig. 2.4a). We then examined the localization and glycosylation states of these mutants. Panx1ΔLRR-EGFP and Panx1ΔHCS-EGFP exhibited drastically decreased surface localization, as determined by cell surface biotinylation (Fig. 2.4b) and confocal imaging (Fig. 2.4c). Additionally, only Gly0 and Gly1 forms were detected for Panx1ΔLRR-EGFP and Panx1ΔHCS-EGFP consistent with restricted cell surface expression (Fig. 2.4d). Conversely, Panx1ΔVS-EGFP exhibited a more subtle but still significant decrease in cell surface expression and had glycosylation profiles similar to full length Panx1-EGFP (Fig. 2.4). Panx1ΔVS-EGFP formed oligomers consistent with those of Panx1-EGFP (Fig. 2.5). Unexpectedly, we detected intermediate bands for Panx1ΔLRR-EGFP and Panx1ΔHCS-EGFP despite their drastic reduction in cell surface localization (and therefore reduced exposure to crosslinker). These intermediates were broader than those detected in Panx1-EGFP and Panx1ΔVS-EGFP samples and were also faintly detectable in samples that had not been exposed to any crosslinker (data not shown).

Together, these data identify a putative LRR motif in the Panx1CT and reveal its critical role in Panx1 cell surface localization.

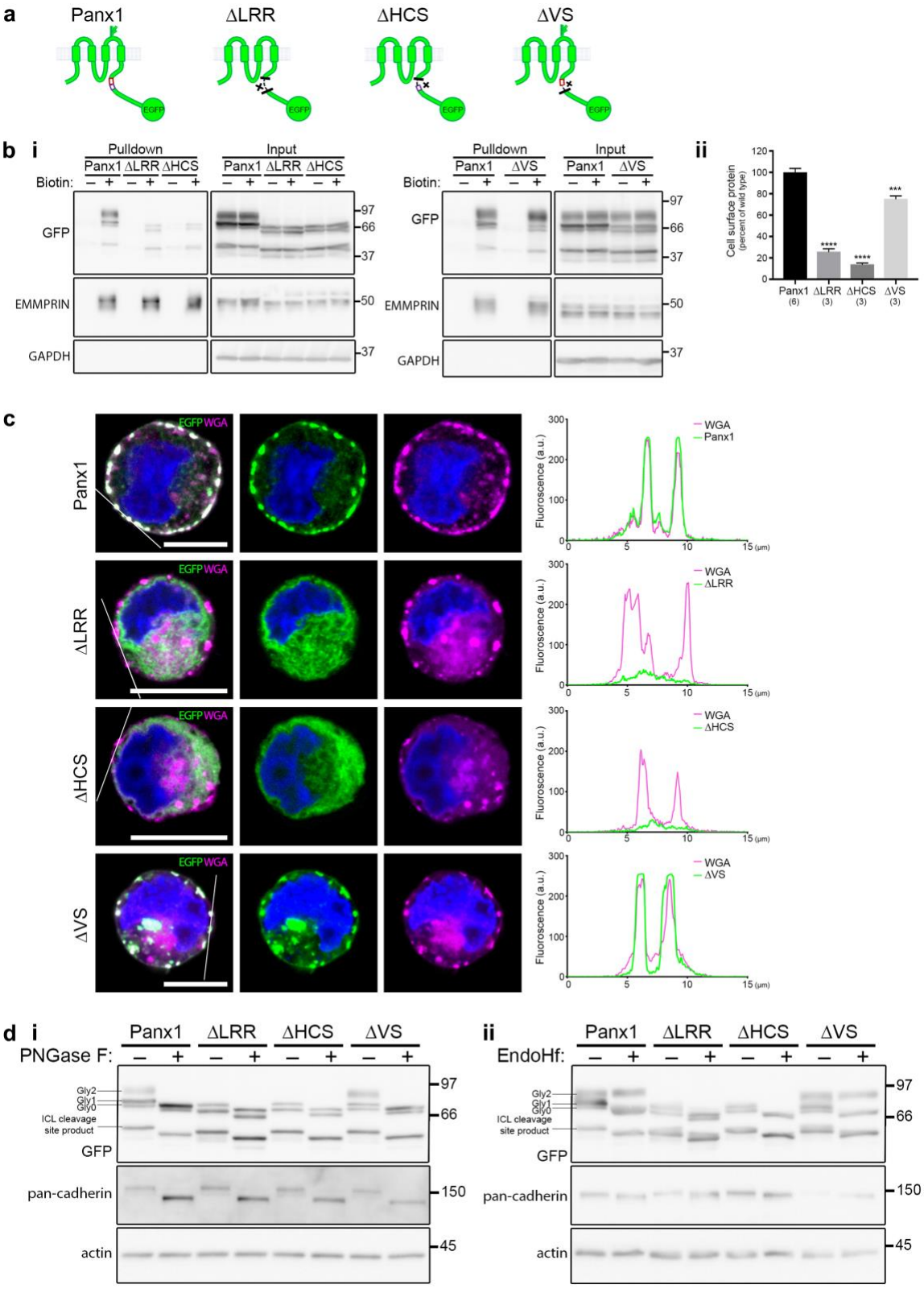
a
Panx1
ΔLRR
ΔHCS
ΔVS
EGFP
b i
Pulldown
Input
Panx1 ΔLRR ΔHCS
Biotin:
GFP
EMMPRIN
GAPDH
97
66
37
50
Panx1 ΔVS
ii
Cell surface protein (percent of wild type)
Panx1 (6)
ΔLRR (3)
ΔHCS (3)
ΔVS (3)
****
***
c
EGFP WGA
Fluorescence (a.u.)
WGA
Panx1
ΔLRR
ΔHCS
ΔVS
d i
PNGase F:
ii
EndoHf:
Gly2
Gly1
Gly0
ICL cleavage site product
GFP
pan-cadherin
actin
150
45

Figure 2.4. A novel putative LRR motif in the Panx1CT is necessary for trafficking Panx1-EGFP to the cell surface.

(a) Schematic of full length Panx1-EGFP and the Panx1ΔLRR-EGFP, Panx1ΔHCS-EGFP, and Panx1ΔVS-EGFP deletion mutants. (b) Cell surface biotinylation assays reveal that the putative LRR motif, or HCS alone, are required for cell surface localization, while the VS is also mildly important. (*i*) Representative Western blot of pulldown (cell surface protein) and input. Anti-EMMPRIN was used as a positive control for biotin pulldown and as a loading control, and anti-GAPDH was used as a negative control against biotin internalization. (*ii*) Panx1ΔLRR-EGFP and Panx1ΔHCS-EGFP exhibited reduced cell surface levels compared to Panx1-EGFP. Surface levels of Panx1ΔVS-EGFP were also reduced compared to those of Panx1-EGFP, though to a lesser degree. Data are presented as mean ± SEM. One-way ANOVA with Dunnett's multiple comparisons test, $N = 3$, $\alpha = 0.05$, $F(3, 11) = 152.4$, ***$p = 0.0007$, ****$p < 0.0001$, ns, nonsignificant. (c) Confocal images of HEK293T cells overexpressing Panx1-EGFP, Panx1ΔLRR-EGFP, Panx1ΔHCS-EGFP, or Panx1ΔVS-EGFP (green). Hoechst was used as a nuclear counterstain (blue) and wheat-germ agglutinin (WGA) was used as a plasma membrane marker (magenta). Overlapping EGFP and WGA signals (white) and line scans through the cell membrane reveal cell surface localizaton of each protein. While both Panx1-EGFP and Panx1ΔVS-EGFP co-distributed with WGA, Panx1ΔLRR-EGFP and Panx1ΔHCS-EGFP did not. N=3. Scale bars, 10 μm. (d) Deglycosylation assays using (*i*) PNGase F or (*ii*) EndoHf reveal Panx1-EGFP and Panx1ΔVS-EGFP exhibited Gly0, Gly1, and Gly2 glycosylation species, while Panx1ΔLRR-EGFP and Panx1ΔHCS-EGFP exhibited only Gly0 and Gly1 forms. Anti-pan-cadherin and anti-β-actin were used as a positive and negative controls for deglycosylation, respectively.

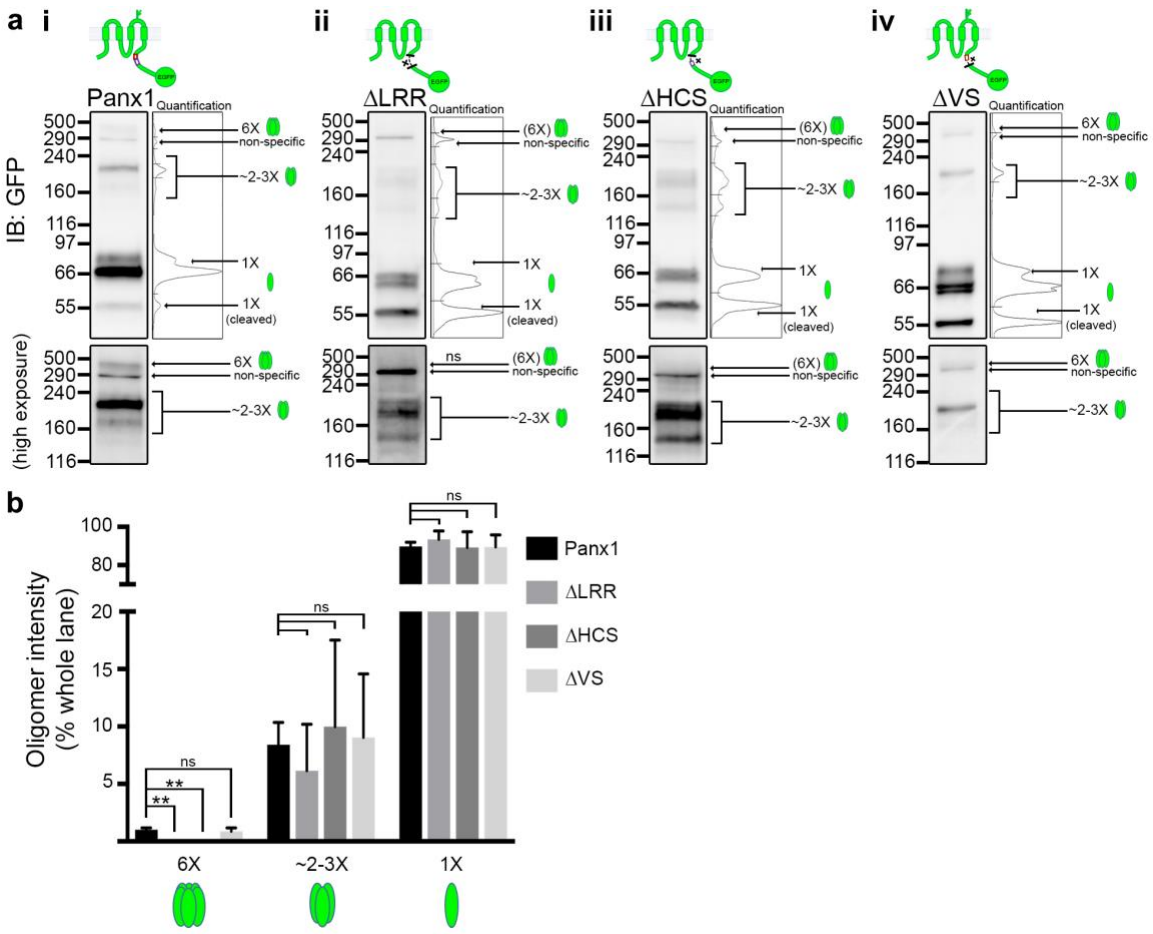

Figure 2.5. Surface hexamers are not detected with complete putative LRR motif or HCS sequence deletion.

(a) Crosslinking assays reveal oligomerization profiles of LRR motif deletion mutants. Representative Western blots observing HEK293T cell lysates post-transfection with (*i*) Panx1-EGFP, (*ii*) Panx1ΔLRR-EGFP, (*iii*) Panx1ΔHCS-EGFP, or (*iv*) Panx1ΔVS-EGFP, and after crosslinking with the cell-impermeable crosslinker, BS^3, to observe surface-localized oligomers (6X or ~2-3X). Higher exposures of the regions (above 116 kDa) were included to better illustrate the presence or absence of high molecular weight bands. (b) Individual oligomeric bands were quantified and expressed as a percentage of the entire GFP signal in each lane. Non-

specific bands were excluded from the analysis. Data are presented as mean ± SEM. One-way ANOVA with Dunnett's multiple comparisons test, $N = 3$, $\alpha = 0.05$, $F(3,8) = 10.59$, $^{**}p = 0.0072$ (6X), ns, nonsignificant.

2.3.3 Panx1-EGFP regulation of HEK293T cell proliferation requires the LRR motif

In a previous study, our group found that expression of Panx1 promoted cell proliferation in N2a cells and primary neural precursor cells (Wicki-Stordeur et al. 2012). Similarly, here we found that transfection with Panx1-EGFP increased HEK293T cell proliferation compared to EGFP-transfected controls (Fig. 2.7a*i-iii*). There were no differences in cell death or viability, as observed by the Trypan blue live/dead cell counts (Fig. 2.7a*iv*) and MTT assay (Fig. 2.7b). Notably, expression of Panx1ΔHCS-EGFP had no effect on HEK293T cell proliferation (Fig. 2.7a*i-iii*). These data support the findings that the HCS within the putative LRR motif is required for functional expression of Panx1 at the cell surface.

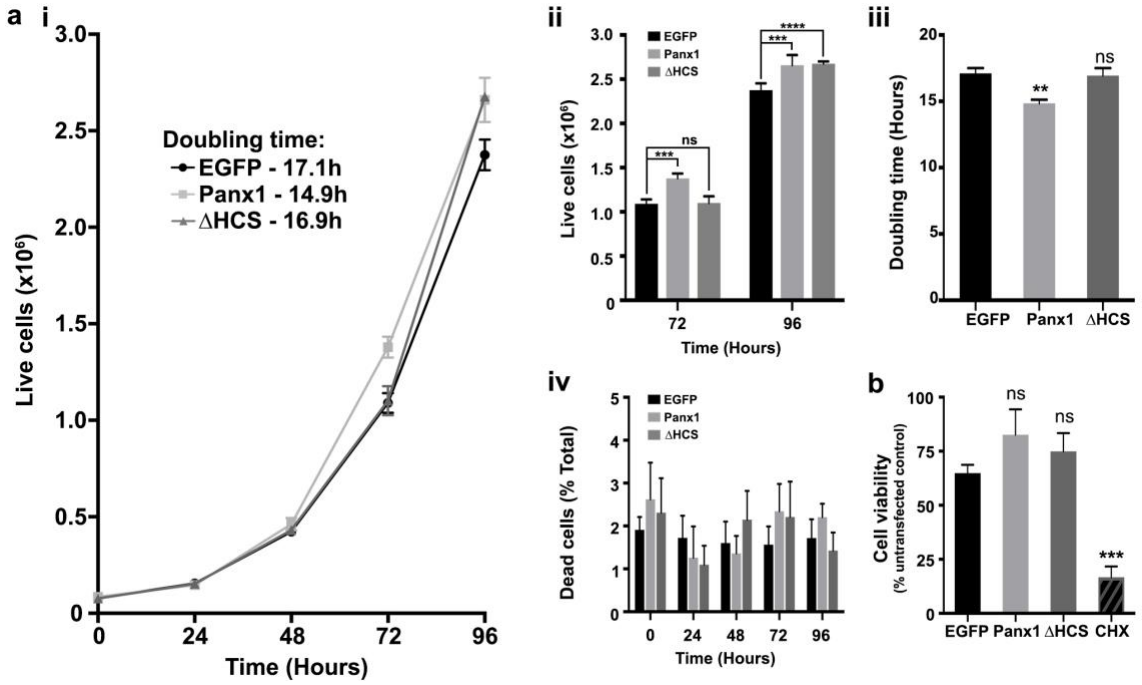

Figure 2.6. Panx1-EGFP overexpression increases HEK293T cell proliferation, but not when it lacks the HCS sequence (Panx1ΔHCS-EGFP).

(a) Trypan blue proliferation assays. (*i*) HEK293T cells overexpressing either Panx1-EGFP, Panx1ΔHCS-EGFP, or EGFP control were counted at 5 time points with the first time point, T0, taking place at 24 h post-transfection (6 h after re-plating). Cell counts were used to plot growth curves. (*ii*) Histogram with cell counts from T0, T72, and T96 identifying significant differences in cell counts at each time point. Data are presented as mean ± SEM. Two-way ANOVA with Dunnett's multiple comparisons test, $N = 4$, $\alpha = 0.05$, $F(2,45) = 8.459$, ***$p = 0.0002$, ****$p < 0.0001$, ns, nonsignificant. (*iii*) Doubling time comparisons of each condition, calculated using data from time points in the exponential growth phase. Data are presented as mean ± SEM. One-way ANOVA with Dunnett's multiple comparisons test, $N = 4$, $\alpha = 0.05$, $F(2,9) = 8.681$, **$p = 0.0079$, ns, nonsignificant. (b) MTT assays performed at T72 on HEK293T cells overexpressing either EGFP, Panx1-EGFP, Panx1ΔHCS-EGFP, or untransfected cells treated with a toxic dose

(200 μg/mL) of cycloheximide (CHX) confirm that differences in cell numbers were not due to alterations in cell viability. Data are presented as the mean percentage of untransfected control ± SEM. One-way ANOVA with Dunnett's multiple comparison's test, $N = 6$, $\alpha = 0.05$, $F(3,20) = 17.35$, ****$p < 0.0001$, ns, nonsignificant.

2.4 Discussion

Discovery of a consensus sequence for a putative LRR motif within the proximal Panx1CT that impacts on Panx1 localization provides new mechanistic insight into the molecular determinants of Panx1 trafficking and localization. These findings also raise several new important questions. For instance, do the HCSs in the Panx1CT contribute to LRR motifs that form a full LRR domain (2 or more repeats in length)? Are LRR motifs or LRR domains found in the other pannexin family members? How does this discovery inform on previously identified homology between Panx1 and LRRC8A? Further, what role do the C-terminal LRR motif and additional LRR HCS sequences play in Panx1 activity? Here we discuss some aspects of the evidence related to these new questions arising from this research.

We observed substantial decreases in cell surface expression as well as the presence of immature glycosylation status with deletion mutants lacking the HCS of the putative LRR motif (Panx1Δ299-EGFP, Panx1ΔLRR-EGFP, and Panx1ΔHCS-EGFP) motif. Conversely, deletion mutants in which the HCS was present (Panx1Δ379-EGFP and Panx1ΔVS-EGFP) were more similar full length Panx1 in regards to localization and glycosylation profiles. Since HCS's usually form β-sheet and VS's often form an α-helix (Ng et al. 2011; Bella et al. 2008; Kajava 1998), we examined whether these secondary structures directly align with the HCS1-HCS5 described in Fig. 2.3 and Table 1, which could help verify the LRR structure(s) in the Panx1CT

and identify corresponding VS. Notably, a previously identified β-strand (Spagnol et al. 2014) aligned with HCS5 (Table 1), though it was not followed by an α-helix. The multiple HCS consensus sequences, the general promiscuity in LRR domain secondary structure (Bella et al. 2008), and the previously identified mixture of α-helices and β-strands (Spagnol et al. 2014) raise the possibility of the existence of an LRR domain within the Panx1CT. Though glycosylation is not a direct indicator of cell surface expression, it can infer the degree of progression through the secretory pathway. The complex N-linked glycosylation (Gly2) typical of Panx1 occurs in the *trans*-Golgi (Stanley 2011), late in the pathway. Consistent with this paradigm, we found that deletion mutants enriched at the cell surface were also complexly glycosylated, while the majority of those exhibiting decreased surface presented with immature glycosylation status. These mutants were still capable of reaching the high-mannose glycosylation species (Gly1), which occurs in the endoplasmic reticulum and can also be identified on proteins in the *cis*-Golgi (Stanley 2011). Interestingly, all deglycosylation enzyme-treated samples exhibited bands that presented 'below' the lowest 'Gly0' band of the untreated sample (actin negative control signals were unaffected). This suggests that even the previously designated Gly0 species of Panx1-EGFP is glycosylated to some degree and requires further study.

This new information on the role of the putative C-terminal LRR motif on Panx1 subcellular distribution has important implications for understanding the functional diversity of all 3 pannexin family members. With respect to the C-termini, the relatively weak homology between the 3 pannexins, compared with the homologies between other domains, suggests that the C-termini likely impart unique aspects to their respective biological roles and regulation (localization, function, interactions, etc.). Panx1 and Panx3 exhibit relatively similar C-termini

(i.e. length, sequence homology) and both proteins traffic to the cell surface; whereas, Panx2 has a much larger C-terminus with low relative sequence homology, and localizes to intracellular compartments (Penuela et al. 2009; Penuela et al. 2013). The Panx1 and Panx3 C-termini are also higher in leucine content than Panx2 (~15-17% compared to 8.8%, respectively). Examination of each sequence revealed multiple regions in the C-termini matching the LRR HCS consensus sequence (Fig. 2.3; Supplementary Fig. S2). It is reasonable to speculate that pannexin intermixing (Penuela et al. 2009; Ambrosi et al. 2010) could involve interactions between larger LRR domains formed by these putative LRR motifs (Bella et al. 2008; Scott et al. 2004; Jin et al. 2007; Deneka et al. 2018; Kefauver et al. 2018).

LRRC8A shares sequence homology with Panx1 from the N-terminus to the fourth transmembrane domain (Deneka et al. 2018; Kefauver et al. 2018; Abascal & Zardoya 2012), and contains LRR domains in its C-terminus, which interact with one another within the hexamer. Notably, the LRRC8A hexamer is formed by a trimer of dimers (Kefauver et al. 2018), reminiscent of the relatively abundant cell surface expressed 'intermediate' Panx1 oligomer (Fig. 2.2a*i*, Fig. 2.5A*i*) corresponding to either a dimer or trimer, previously detected in whole cell lysates (Boassa et al. 2007; Chiu et al. 2017). Previous homology analysis between LRRC8A and Panx1 focused on the N-terminus to the fourth transmembrane domain (Abascal & Zardoya 2012). Our findings suggest that the degree of homology between C-termini could also be of interest. Based on the cell surface crosslinking data, it is tempting to speculate that Panx1 forms intermediate oligomers that are stable at the cell surface.

As the Panx1CT regulates Panx1 activity (reviewed in Boyce et al. 2018, Chiu et al. 2018, Dahl 2018), our discovery of a putative LRR motif in the Panx1CT could have functional implications. Several studies suggest that the C-terminus interacts with the Panx1 channel pore in

an autoinhibitory manner (Wang & Dahl 2010; Sandilos et al. 2012). One group proposed a model in which a region in the Panx1CT, I360-G370, interacts with membranes, and that this interaction facilitates Panx1CT insertion into the pore of Panx1 (Spagnol et al. 2014). Interestingly, one of the HCS consensus sequences we highlighted, HCS4, almost directly overlaps with the suggested membrane-interacting region (Table 1). Further, HCS3 contains a cysteine group that was implicated in channel gating (Wang & Dahl 2010), and HCS5 overlaps with the Panx1CT caspase-cleavage site which activates Panx1 (Chekeni et al. 2010; Sandilos et al. 2012).

Overall, the discovery of the putative LRR motif within the Panx1CT broadens our understanding of the molecular determinants of Panx1 trafficking and localization. This work also raises important new questions with respect to the regulation and functional implications of Panx1 oligomerization state at the cell surface.

Table 2.1. HCS consensus sequences in the Panx1CT.

A list of amino acid sequences in the Panx1CT that match the broad LRR consensus rules: LxxLxLxxNxL or LxxLxLxxCxxL, where L is usually Leu, Iso, Val, or Phe (but can also be any hydrophobic amino acid); N is Cys, Ser, Thr, or Asn; C is Cys, Ser, or Asn; and x is any residue. Additionally, the first and last L in the sequence can be replaced by relatively hydrophilic residues. The putative LRR examined in this study is boldly outlined.

Designated HCS number	Discovered by ScanProsite or by visual inspection?	Amino acids	Consensus sequence LxxLxLxxNxL LxxLxLxxCxxL	Overlapping sites of interest
HCS1	Visual inspection	L305-L315	**L**kv**Y**e**I**lp**T**f**D**	Endocytic recognition sequence (Y308-L311)(Boyce et al. 2014) Phosphorylation site (Y308)(Weilinger et al. 2016)
HCS2	ScanProsite	L329-E340	**L**yn**L**f**L**ee**N**i**S** or **L**yn**L**f**L**ee**N**is**E**	Endocytic recognition sequence (Y330-F333)(Boyce et al. 2014)
HCS3	Visual inspection	Y344-S355	**Y**kc**L**k**V**le**N**i**K** or **Y**kc**L**k**V**le**N**ik**S**	Endocytic recognition sequence (Y344-L347)(Boyce et al. 2014) Channel gating, S-Nitrosylation site (C346)(Lohman, Weaver, et al. 2012; Wang & Dahl 2010)
HCS4	Visual inspection	I360-M371	**I**dp**M**l**L**lt**N**l**G** or **I**dp**M**l**L**lt**N**lg**M**	Putative membrane-interacting domain (I360-G370)(Spagnol et al. 2014)
HCS5	Visual inspection	I376-T387	**I**id**G**k**I**pt**S**l**Q** or **I**id**G**k**I**pt**S**lq**T**	Caspase-cleavage site (D375-D378)(Chekeni et al. 2010; Sandilos et al. 2012) β-strand (K373-D380)(Spagnol et al. 2014)

2.5 Methods

2.5.1 Plasmids

The mouse Panx1-EGFP plasmid (Penuela et al. 2007) used in this study was a generous gift from Drs. Dale Laird and Silvia Penuela. Deletion mutants were generated using multiple rounds of PCR/overlap PCR followed by restriction digest and ligation into a vector backbone as previously described (Wicki-Stordeur et al. 2013). Briefly, overlap-extension PCR fragments were obtained from Panx1-EGFP using primers specific to regions up- and down-stream from the Panx1 gene and primers specific to regions on either side of the deletion site. The fragments

were gel purified using the QIAquick Gel Extraction Kit (Qiagen Sciences) and overlap-extension PCR was performed using the obtained fragments and primers for regions peripheral to the gene. The resulting PCR product was cloned into pEGFP-N1 vector. The last amino acid in the Panx1Δ299-EGFP mutant is F298. The last amino acid in the Panx1Δ379-EGFP mutant is D378. All constructs were confirmed by sequencing (Eurofins MWG Operon).

2.5.2 Cell culture and transfection

Human Embryonic Kidney (HEK)-293T cells (ATCC) were cultured in Dulbecco's modified Eagle's medium (DMEM) supplemented with 10% FBS, 100 U/mL penicillin, and 100 μg/mL streptomycin (all from Gibco/Life Technologies). Cells were transfected with 7.5 mM linear polyethylenamine (PEI) (Polysciences, Cat. #23966) at a 10:1 PEI (μL):DNA (μg) ratio.

2.5.3 Antibodies

Primary antibodies: anti-β-actin (1:16,000; Sigma), anti-EMMPRIN (1:1000; R&D Systems), anti-GAPDH (1:6000; Novus Biologicals), anti-GFP mouse monoclonal (1:4000; Proteintech), anti-GFP rabbit polyclonal (1:32,000; Molecular Probes), and anti-pan-cadherin (1:1000; Cell Signaling Technology). Secondary antibodies: horseradish peroxidase (HRP)-conjugated AffiniPure anti-rabbit immunoglobulin G (IgG), HRP-conjugated AffiniPure anti-mouse IgG, and HRP-conjugated AffiniPure anti-goat (all at 1:8000; Jackson ImmunoResearch).

2.5.4 Protein extractions and Western blot

Proteins were extracted and analyzed by Western blot as previously described (Wicki-Stordeur & Swayne 2013; Wicki-Stordeur et al. 2012; Swayne et al. 2010). Unless otherwise specified, cells were harvested 48-h post-transfection by scraping in PBS 1% IGEPAL (10 mM PBS [150 mM

NaCl, 9.1 mM Na_2HPO_4, 1.7 mM NaH_2PO_4], 1% IGEPAL CA-630) supplemented with protease inhibitor cocktail at 1 μL/10^6 cells (stock: 0.104 mM 4-(2-aminoethyl)benzenesulfonyl fluoride hydrochloride, 0.08 mM aprotinin, 4 mM bestatin hydrochloride, 1.4 mM N-(trans-epoxysuccinyl)-L-leucine 4-guanidinobutylamide, 2 mM leupeptin hemisulfate salt, 1.5 mM pepstatin-A; Sigma), 0.2 mM PMSF, 10 μM sodium orthovanadate, and 1 mM EDTA and incubated on ice for 30 min. Homogenates were centrifuged 20 min at 12,000 rpm, and supernatants were collected. Samples were heated 5 min at 95˚C in the presence of 1X sample buffer and reducing agents (10% β-mercaptoethanol (BME) and 100 mM dithiothreitol (DTT)) prior to loading on an SDS-PAGE gel. Gels were 4-20% gradient gels (BioRad) for crosslinking assays, or 10% Laemmli gels for all other assays. Protein was transferred to a 0.2 μm pore-size polyvinyldene fluoride (PVDF; BioRad) membrane. Membrane incubations were performed in 5% skim milk powder in PBS-T (10 mM Na_2HPO_4, 1.25 mM NaH_2PO_4, 2.7 mM KCl, 137 mM NaCl, 0.1% Tween-20). Blots were quantified by densitometry using ImageJ (http://imagej.nih.gov/ij/).

2.5.5 Deglycosylation assays

Deglycosylation assays were performed using either PNGase F or EndoH_f (NEB) according to the manufacturer's protocol. Mouse anti-GFP (Proteintech) was used to detect proteins of interest.

2.5.6 Cell surface biotinylation

Cells were washed twice with ice cold biotinylation buffer (137mM NaCl, 2.7 mM KCl, 1.8 mM KH_2PO_4, 10 mM Na_2HPO_4, 0.5 mM $MgCl_2$, 1 mM $CaCl_2$; pH 7.4) then incubated in either 0.25

mg/mL EZ-Link™ Sulfo-NHS-SS-Biotin (Thermo Scientific) in biotinylation buffer or buffer alone (negative control) for 30 min at 4˚C with gentle rocking. The reaction was quenched by adding 1 M glycine in biotinylation buffer to an end concentration of 100 mM glycine, then washing the cells twice (quick) and once for 15 min at 4˚C with gentle rocking in 100 mM glycine in biotinylation buffer. The solution was removed and lysates were prepared as described above, using TBS 1% IGEPAL (50 mM Tris, 150 mM NaCl, 1% IGEPAL CA-630; pH 7.5) and the aforementioned protease inhibitors as lysis buffer. As a preclearing step, lysates were incubated with a 50% slurry of 50 µL of iminobiotin agarose beads (Pierce) for 1 h at 4˚C on with rotation. To isolate cell surface biotinylated proteins, 200-500 µg of total protein was incubated with 50% slurry of 50 µL of NeutrAvidin™ agarose beads (Thermo Scientific) for 2 h at 4˚C with rotation. The beads were washed 4 times with TBS 1% IGEPAL, 4 times with high salt TBS 1% IGEPAL (50 mM Tris, 300 mM NaCl, 1% IGEPAL CA-630; pH 7.5), and twice with 50 mM Tris pH 7.5. Surface biotinylated proteins were eluted for 5 min at 95˚C on a heat block in 1X sample buffer and reducing agents (100 mM DTT and 10% BME). Eluates and inputs were analyzed by Western blot.

2.5.7 Fixed cell imaging

Cells were plated onto poly-D-lysine (PDL; Sigma)-coated coverslips, 24 h post-transfection. To restrict observations to mature proteins, protein translation was briefly inhibited using 20 µg/mL cycloheximide (CHX; Sigma) for 8 h the following day, prior to fixation. Directly before fixation cells were incubated with an AlexaFluor-647-conjugated cell surface marker wheat germ agglutinin (WGA; 5 µg/mL; Molecular Probes) in Hank's Balanced Salt Solution (HBSS, Gibco) for 5 min at 37˚C. Cells were quick-washed in phosphate buffered saline (PBS; 154 mM NaCl,

6.25 mM sodium phosphate monobasic, 18.75 mM sodium phosphate dibasic, pH 7.2), fixed with 4% paraformaldehyde (PFA) in PBS for 10 min, and washed thrice in PBS with the second wash containing Hoechst 33342 (1:300; Thermo Scientific) nuclear counterstain. Coverslips were mounted in VectaShield mounting medium (Vector Laboratories, Inc.). Images were acquired with a Leica TCS SP8 confocal microscope at 2.5X optical zoom (1840 x 1840, pixel area 63 nm^2, 40X (1.3 NA) oil immersion objective) as confocal z-stacks. Representative images were adjusted using Adobe Photoshop (CC 2018, 19.1.1).

2.5.8 BS^3 crosslinking assays

To observe mature protein (enriched at the cell surface), transfected cells were treated with 20 μg/mL CHX for 8 h prior to crosslinking. Cells were washed with ice-cold crosslinking buffer (20 mM PBS [150 mM NaCl, 18.6 mM Na_2HPO_4, 1.4 mM NaH_2PO_4], 1 mM $CaCl_2$, 0.5 mM $MgCl_2$; pH 8), and incubated in either 3 mM bis(sulfosuccinimidyl)suberate (BS^3; Thermo Fisher Scientific) in crosslinking buffer or buffer alone for 30 min on ice. The reaction was quenched by adding 1 M Tris to an end concentration of 20 mM, then incubating in quenching solution (20 mM Tris, 20 mM PBS [150 mM NaCl, 13.7 mM Na_2HPO_4, 6.3 mM NaH_2PO_4], 1 mM $CaCl_2$, 0.5 mM $MgCl_2$; pH 7.2) for 15 min on ice. The solution was removed and lysates were prepared and analyzed by Western blot as described above.

2.5.9 Trypan blue proliferation and MTT assays

Cells were transfected as described above and, at 18 h post-transfection, replated onto 35 mm dishes at $1x10^5$ cells/dish for Trypan blue proliferation assays or in 96-well plates at $1x10^4$ cells/well for MTT assays. Cells were counted every 24 h for 5 days (T0-96), with T0 occurring at 24 h post-transfection. Doubling time was calculated [$DT = T * \ln 2 / \ln(N_{T=1}/N_{T=2})$] using time

points within the linear logarithmic growth curve. MTT assays were performed at T72 using the Vybrant® MTT Cell Proliferation Assay Kit (Thermo Fisher Scientific), according the manufacturer's protocol.

2.5.10 Statistical analysis

Statistical analysis was performed using Prism 7 (GraphPad Software). The tests and P values for each experiment are described in figure legends.

2.6 Supplementary Information

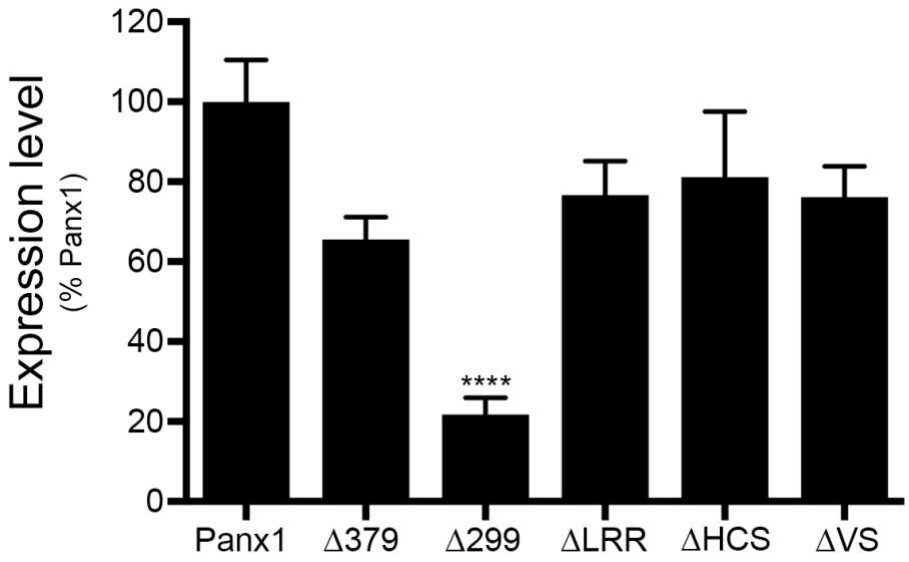

Figure 2.7. (Supplementary Figure S1) Expression levels of all Panx1 deletion mutants. Expression levels were determined from the input lanes of cell surface biotinylation Western blot analyses. Signals from anti-GFP (protein of interest) and anti-EMMPRIN (positive and loading control) were quantified, normalized, and expressed as percent of full length Panx1-EGFP. Data are presented as mean ± SEM. One-way ANOVA with Dunnett's multiple comparisons test, $N = 6$, $\alpha = 0.05$, $F(5,42) = 5.152$, ****$p < 0.0001$.

a Panx2CT

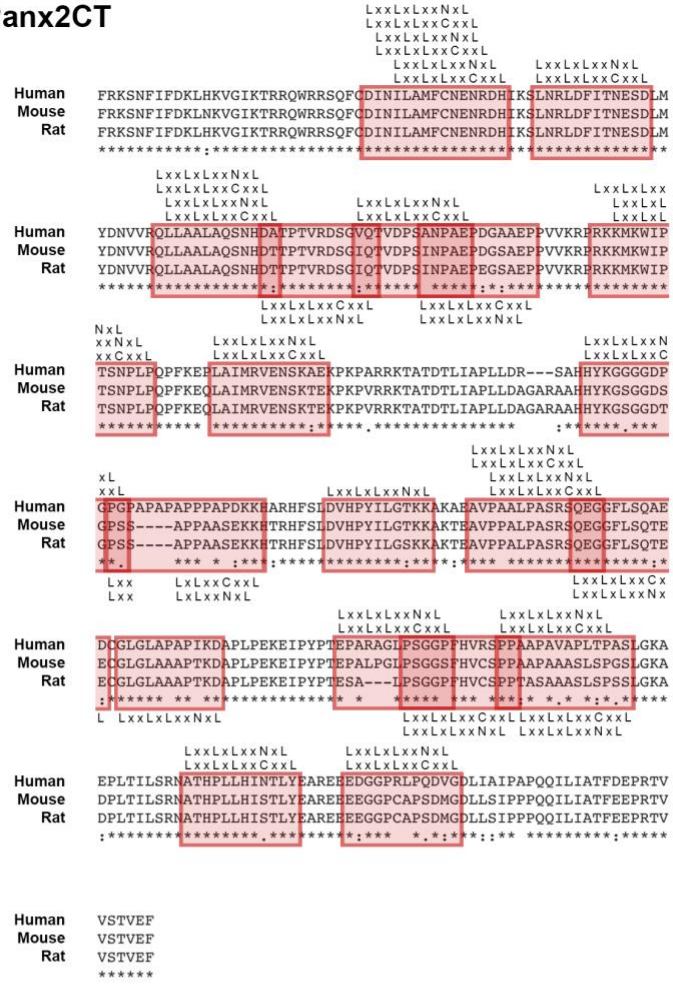

b Panx3CT

Consensus sequence criteria:

Sequence: LxxLxLxxNxL
OR
LxxLxLxxCxxL

where: L = I, V, L, or F
N = C, S, T, or N
C = C, S, or N
x = any residue

"L"s are sometimes any other hydrophobic residue (G, A, P, C, M, Y, W)
first and last "L" can be hydrophilic (R, H, K, D, E, S, T, N, Q)

Figure 2.8. (Supplementary Figure S2) HCS consensus sequences in the C-termini of other pannexin family members.

Sequence alignment of (A) Panx2CT and (B) Panx3CT using sequences from human, mouse, and rat, with regions of each identified HCS highlighted in red. The alignment was generated in CLUSTAL O (1.2.3) using NCBI accession numbers: NP_443071.2 (human), NP_001002005.2 (mouse), and NP_955441.2 (rat) for Panx2, and NP_766042.1 (human), NP_4431931.1 (mouse), and NP_955430.1 (rat) for Panx3.

3. General discussion

The data presented in this manuscript-based thesis provided new insights into mechanisms of trafficking of Panx1, and ion channels in general. The resulting working model is that the LRR sequence identified in the Panx1CT may form an LRR motif, which is necessary for cell surface localization of Panx1 (Fig. 3.1). While this thesis confirmed that this region is involved in Panx1 trafficking, it is also possible that it plays a role in the regulation of Panx1 oligomerization and/or activity (Fig. 3.2). In addition, proliferation assays further showcase Panx1 as an ion channel with diverse influences on behaviour in a variety of cell types. Looking beyond Panx1, this work also provides insights into mechanisms by which LRRs may regulate ion channels and protein trafficking, a subject that is at this time poorly understood. In this chapter, I discuss the questions and implications that arise from these findings, as well as future directions that would expand on our current knowledge regarding regulation of Panx1.

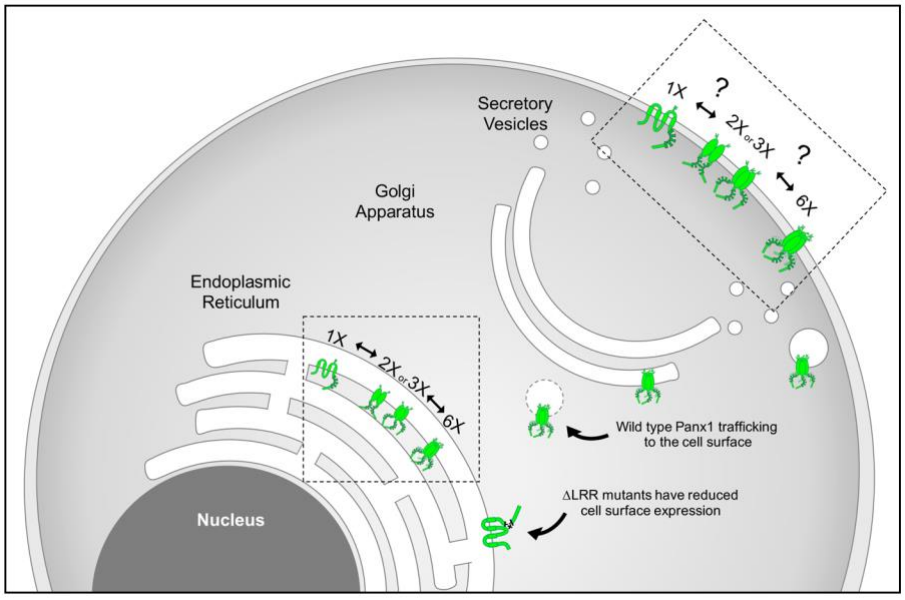

Figure 3.1. Working model.

A putative LRR motif identified in the Panx1CT is necessary for cell surface localization of Panx1. Meanwhile, the crosslinking data in this thesis raises questions in regards to the mechanisms of Panx1 oligomerization (dotted outlines). Whether Panx1 channels form intermediate oligomers somewhere en route to the plasma membrane, whether intermediates precede formation of the hexamer, whether Panx1 can toggle between intermediate and hexameric form, and whether these intermediates are functional in some way, remains to be determined.

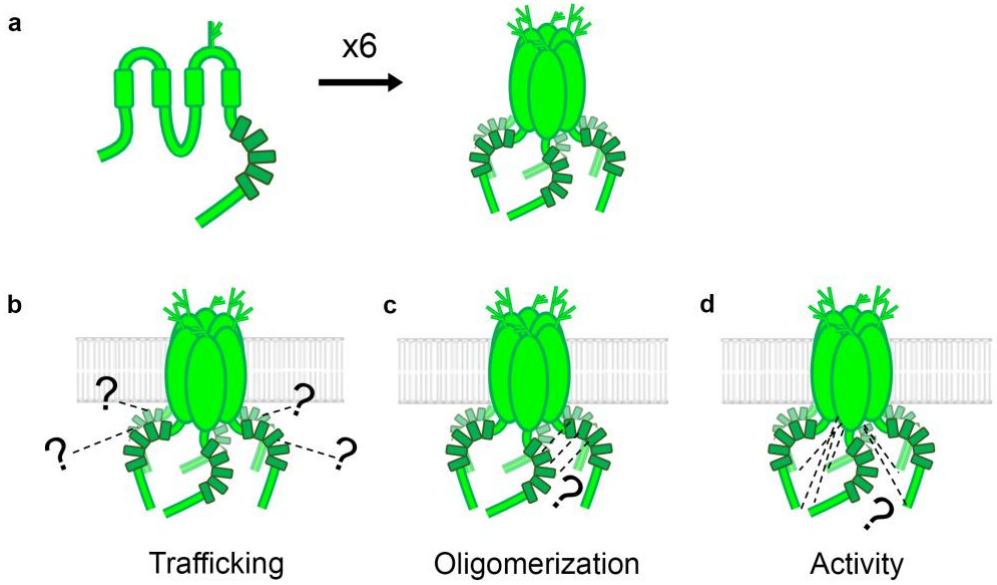

Figure 3.2. Other potential roles of an putative LRR domain in the Panx1CT.

(a) Schematic of Panx1 hexamer formation, with a theoretical LRR domain in the Panx1CT. The LRR domain is illustrated with 5 repeats, as I discovered 5 HCS consensus sequences in the Panx1CT. If an LRR domain (2 or more repeats in length) does indeed form in the Panx1CT, it may not use all 5 of the identified HCS. Of note, this study only observed effects of modifying the 'second' LRR (consisting of HCS2 and a VS identified by ScanProsite (de Castro et al. 2006)). (b) The putative LRR/LRR domain regulates trafficking of Panx1, likely through

interactions with important trafficking partners (indicated by question marks). This effect was confirmed in this study, which showed that one of the LRRs (which may function as or contribute to formation of an LRR domain) was required for cell surface localization of Panx1. (c) The putative LRR/LRR domain may regulate Panx1 oligomerization. As LRRs interact with other LRRs, this region may be involved in formation of oligomers. As the crosslinking assays in this study only observed cell surface oligomers and as Panx1 deletion mutants lacking an intact LRR motif had decreased cell surface expression, future work will focus on how this region influences Panx1 oligomerization. (d) The putative LRR/LRR domain may regulate Panx1 activity. Previous work suggests that the Panx1CT interacts with the pore of the channel in an autoinhibitory manner. If intra/intermolecular interactions of the putative LRR motif/LRR domain(s) in the Panx1CT are altered, this could result in dislodging of the C-terminus from the pore and consequent Panx1 activation. Validation of such interactions will undoubtedly be the focus of future work.

3.1 The LRR, a new factor in cell surface expression of transmembrane proteins/ion channels?

This study provides insights into regulatory mechanisms of ion channel trafficking. While I observed that deletion of an LRR motif sequence in Panx1 resulted in a loss of cell surface expression, interference assays with peptidomimetics that resemble each putative LRR motif might serve as a complementary approach to confirm involvement of LRR motif sequence in Panx1 trafficking. This approach assumes that the peptides would directly disrupt important interactions necessary for the trafficking of Panx1 to the cell surface and therefore preclude the channel's cell surface localization. As Panx1 has previously been found to interact with a variety

of other proteins, it would be useful to determine whether Panx1-protein interactions are altered when the LRR/LRR domain is disrupted. Particularly interesting would be the interactions of the Panx1CT with actin, which has been proposed to be related to Panx1 surface expression, based on actin's role at the cell periphery (Bhalla-Gehi et al. 2010).

Another open question is the precise localization of our deletion mutants retained inside the cell. The expression level of our Panx1CT full deletion mutant (Panx1Δ299-EGFP) was similar to a previous report, where Panx1Δ307-RFP was expressed at lower levels than wild type and was trafficked to the proteasome for degradation (Gehi et al. 2011). While our similar mutant, Panx1Δ299-EGFP, also exhibited significantly lower expression levels, other mutants that did not reach the cell surface (Panx1ΔLRR-EGFP and Panx1ΔHCS-EGFP) did not demonstrate evidence of degradation. Future studies using markers for intracellular compartments could shed light on the localization of these mutants, which could provide hints as to when and where the suggested LRR-mediated trafficking of Panx1 occurs.

This work contributes to our understanding of LRR motifs and the trafficking of ion channels in general. LRR domains are best known for their ability to mediate interactions between the LRR-containing protein and other molecules. Further, the majority of membrane protein LRRs reported thus far are located in extracellular regions. Having identified a putative LRR within the intracellular Panx1CT furthers our understanding of the role of LRRs as diverse and variable motifs. In addition, this new information will also increase our ability to identify such regions by strengthening the power of bioinformatics tools used to recognize the motif, should the structure of LRR motif and/or LRR domain be confirmed in the Panx1CT in the future (i.e. via X-ray crystallography).

3.2 Do multiple LRRs in the Panx1CT form an LRR domain?

In this thesis, I investigated the subcellular localization of Panx1 when a single putative LRR motif in the Panx1CT – the LRR that was identified by ScanProsite (containing "HCS2" and the identified VS) – was deleted. I confirmed that this LRR motif sequence is a necessary component in the Panx1CT for surface expression of the protein. However, it is unclear whether this single putative LRR motif regulates trafficking of the protein independently or if its deletion simply disrupts the formation of a larger LRR domain formed by the other identified HCS motifs. In other words, are any of the other HCS consensus sequences (identified by visual inspection; HCS1, HCS3-5) involved in forming LRR motifs, and/or an LRR domain (2 or more repeats in length)? Or does the single LRR motif function as an LRR domain, even though it is only one repeat in length?

Future work will aim to further validate the structure of both single LRR motifs and a larger LRR domain in the Panx1CT. Perhaps most useful would be the acquisition of a 3-dimensional structure of Panx1 or its C-terminus alone so as to directly observe the secondary and tertiary structures of the Panx1CT. Another useful study would be to disrupt aspects of the putative LRR motif consensus sequence by site-directed mutagenesis, rather than deletions of entire regions. Specifically, mutation of the conserved hydrophobic leucine residues found in the HCS to alanine groups or bulky hydrophilic residues would be a good approach. This could disrupt the ability of the Panx1CT to form repeats and/or an LRR domain, and thus disrupt its interactions with partners potentially crucial for cell surface localization. These changes should be applied not only to the LRR HCS that was deleted in this study, but to each identified HCS, which, along with their unidentified VS residues, may collectively form an LRR domain. Finally, while this study suggests that the LRR motif is necessary for cell surface localization, it would also be helpful to test whether the region is sufficient for cell surface localization. A study of an LRR-EGFP construct – i.e. the LRR region ligated to EGFP – would be a good way to

address this. If this construct alone trafficked to the cell surface, this data would support the role of the LRR in cell surface localization of Panx1.

3.3 Role of an LRR/LRR domain in Panx1 activity?

As the Panx1CT has been implicated in regulation of Panx1 activity (reviewed in Boyce et al. 2015; Chiu et al. 2018; Dahl 2018), our discovery of a putative LRR motif in the Panx1CT has implications for Panx1 activity. Several studies suggest that the C-terminus interacts with and auto-inhibits the channel pore (Wang & Dahl 2010; Sandilos et al. 2012; reviewed in Chiu et al. 2018; Dahl 2018). One group proposed a model in which a hydrophobic region in the Panx1CT, residues I360-G370, interacts with membranes, and that this interaction facilitates Panx1CT insertion into the pore of Panx1 (Spagnol et al. 2014). Interestingly, one of the HCS consensus sequences we highlighted, HCS4, almost directly overlaps with the predicted membrane-interacting region (see Table 2.1). Further, HCS3 contains a cysteine group that was implicated in channel gating (Wang & Dahl 2010) and HCS5 overlaps with the Panx1CT caspase-cleavage site which activates Panx1 (Chekeni et al. 2010; Sandilos et al. 2012).

The mechanisms of Panx1 activation are complex, and typically observed using tools that require cell surface localization of the channel such as electrophysiology, ATP release assays, or related dye flux assays. As the LRR deletion mutants in this study had reduced cell surface localization, this study did not observe functional assays of the deletion mutants. However, my proliferation assays suggest that expression of Panx1 lacking the HCS of the putative LRR motif (Panx1ΔHCS-EGFP) is not able to increase proliferation to the same extent as full length Panx1. One potential mechanism for Panx1-stimulated proliferation is via increased activation of purinergic receptors (Wicki-Stordeur et al. 2012). As the Panx1ΔHCS-EGFP mutant exhibited

significantly reduced cell surface expression compared to wild type, its ability to mediate ATP release and thus stimulate purinergic signaling pathways would presumably have been lessened compared to full length Panx1-EGFP. However, it is possible that other mechanisms requiring an intact LRR motif/LRR domain in the Panx1CT are a prerequisite for this effect on proliferation, and future work should address this outstanding question.

Overall this work provides further insight into the localization, oligomerization, and cell physiological roles of an important membrane protein, Panx1, while also furthering our knowledge of the potential roles of LRR motifs and/or domains in ion channel trafficking.

Bibliography

Abascal, F. & Zardoya, R., 2012. LRRC8 proteins share a common ancestor with pannexins, and may form hexameric channels involved in cell-cell communication. *BioEssays*, 34(7), pp.551–560.

Abbracchio, M.P. et al., 2009. Purinergic signalling in the nervous system: an overview. *Trends in Neurosciences*, 32(1), pp.19–29. Available at: http://www.ncbi.nlm.nih.gov/pubmed/19008000.

Vanden Abeele, F. et al., 2006. Functional implications of calcium permeability of the channel formed by pannexin 1. *J Cell Biol*, 174(4), pp.535–546.

Ambrosi, C. et al., 2010. Pannexin1 and Pannexin2 channels show quaternary similarities to connexons and different oligomerization numbers from each other. *J Biol Chem*, 285(32), pp.24420–24431.

Andrade, M.A. et al., 2000. Homology-based method for identification of protein repeats using statistical significance estimates. *Journal of Molecular Biology*, 298(3), pp.521–537.

Andrews, R.K. & Berndt, M.C., 2004. Platelet physiology and thrombosis. In *Thrombosis Research*. pp. 447–453.

Ardiles, A.O. et al., 2014. Pannexin 1 regulates bidirectional hippocampal synaptic plasticity in adult mice. *Front Cell Neurosci*, 8, p.326. Available at: http://www.ncbi.nlm.nih.gov/pubmed/25360084.

Bao, L., Locovei, S. & Dahl, G., 2004. Pannexin membrane channels are mechanosensitive conduits for ATP. *FEBS Lett*, 572(1–3), pp.65–68.

Baranova, A. et al., 2004. The mammalian pannexin family is homologous to the invertebrate innexin gap junction proteins. *Genomics*, 83(4), pp.706–716.

Bargiotas, P. et al., 2012. Functional outcome of pannexin-deficient mice after cerebral ischemia. *Channels*, 6(6), pp.453–456. Available at: http://www.ncbi.nlm.nih.gov/pubmed/23111424.

Bargiotas, P. et al., 2011. Pannexins in ischemia-induced neurodegeneration. *Proceedings of the National Academy of Sciences of the United States of America*, 108(51), pp.20772–7. Available at: http://www.pubmedcentral.nih.gov/articlerender.fcgi?artid=3251101&tool=pmcentrez&rendertype=abstract.

Baroja-Mazo, A., Barberà-Cremades, M. & Pelegrín, P., 2013. The participation of plasma membrane hemichannels to purinergic signaling. *Biochimica et Biophysica Acta - Biomembranes*, 1828(1), pp.79–93.

Beckmann, A. et al., 2016. Pannexin-1 channels show distinct morphology and no gap junction characteristics in mammalian cells. *Cell and Tissue Research*, 363(3), pp.751–763.

Bella, J. et al., 2008. The leucine-rich repeat structure. *Cellular and Molecular Life Sciences*, 65(15), pp.2307–2333.

Bhalla-Gehi, R. et al., 2010. Pannexin1 and pannexin3 delivery, cell surface dynamics, and cytoskeletal interactions. *J Biol Chem*, 285(12), pp.9147–9160. Available at: http://www.ncbi.nlm.nih.gov/entrez/query.fcgi?cmd=Retrieve&db=PubMed&dopt=Citation&list_uids=20086016.

Billaud, M. et al., 2015. A molecular signature in the pannexin1 intracellular loop confers channel activation by the α1 adrenoreceptor in smooth muscle cells. *Science signaling*, 8(364), p.ra17.

Billaud, M. et al., 2011. Pannexin1 regulates α1-adrenergic receptor- mediated vasoconstriction.

Circulation Research, 109(1), pp.80–85.

Boassa, D. et al., 2007. Pannexin1 channels contain a glycosylation site that targets the hexamer to the plasma membrane. *J Biol Chem*, 282(43), pp.31733–31743. Available at: http://www.ncbi.nlm.nih.gov/entrez/query.fcgi?cmd=Retrieve&db=PubMed&dopt=Citation&list_uids=17715132.

Bou Khalil, M. et al., 2010. Lipidomics era: Accomplishments and challenges. *Mass Spectrometry Reviews*, 29(6), pp.877–929.

Boyce, A.K. et al., 2015. ATP stimulates pannexin 1 internalization to endosomal compartments. *Biochem J*, 470(3), pp.319–330. Available at: http://www.ncbi.nlm.nih.gov/pubmed/26195825.

Boyce, A.K. et al., 2014. Pore positioning: current concepts in Pannexin channel trafficking. *Channels (Austin)*, 8(2), pp.110–117. Available at: http://www.ncbi.nlm.nih.gov/pubmed/24300303.

Boyce, A.K.J. et al., 2018. Transcriptional and post-translational regulation of pannexins. *Biochimica et Biophysica Acta (BBA) - Biomembranes*, 1860(1), pp.72–82. Available at: https://linkinghub.elsevier.com/retrieve/pii/S0005273617300780.

Boyce, A.K.J. & Swayne, L.A., 2017. P2X7 receptor cross-talk regulates ATP-induced pannexin 1 internalization. *Biochemical Journal*, 474(13), pp.2133–2144. Available at: http://biochemj.org/lookup/doi/10.1042/BCJ20170257.

Bravo, D. et al., 2014. Pannexin 1: A novel participant in neuropathic pain signaling in the rat spinal cord. *Pain*, 155(10), pp.2108–2115.

Bruzzone, R. et al., 2003. Pannexins, a family of gap junction proteins expressed in brain. *Proc Natl Acad Sci U S A*, 100(23), pp.13644–13649.

Burma, N.E. et al., 2017. Blocking microglial pannexin-1 channels alleviates morphine withdrawal in rodents. *Nature Medicine*, 23(3), pp.355–360. Available at: http://www.nature.com/doifinder/10.1038/nm.4281.

Burnstock, G. et al., 2011. Purinergic signalling: from normal behaviour to pathological brain function. *Progress in neurobiology*, 95(2), pp.229–274. Available at: http://www.ncbi.nlm.nih.gov/pubmed/21907261.

Burnstock, G., 2016. Purinergic Signalling and Neurological Diseases: An Update. *CNS Neurol Disord Drug Targets*. Available at: http://www.ncbi.nlm.nih.gov/pubmed/27658510.

de Castro, E. et al., 2006. ScanProsite: Detection of PROSITE signature matches and ProRule-associated functional and structural residues in proteins. *Nucleic Acids Research*, 34(WEB. SERV. ISS.), pp.362–365.

Chekeni, F.B. et al., 2010. Pannexin 1 channels mediate "find-me" signal release and membrane permeability during apoptosis. *Nature*, 467(7317), pp.863–867. Available at: http://www.ncbi.nlm.nih.gov/entrez/query.fcgi?cmd=Retrieve&db=PubMed&dopt=Citation&list_uids=20944749.

Chen, Y. et al., 2006. AMIGO and friends: An emerging family of brain-enriched, neuronal growth modulating, type I transmembrane proteins with leucine-rich repeats (LRR) and cell adhesion molecule motifs. *Brain Research Reviews*, 51(2), pp.265–274.

Chiu, Y.-H. et al., 2018. Revisiting multimodal activation and channel properties of Pannexin 1. *The Journal of General Physiology*, 150(1), pp.19–39. Available at: http://www.jgp.org/lookup/doi/10.1085/jgp.201711888.

Chiu, Y.H. et al., 2017. A quantized mechanism for activation of pannexin channels. *Nature Communications*, 8.

Chou, P.Y. & Fasman, G.D., 1978. Empirical predictions of protein conformation. *Annual review of biochemistry*, 47, pp.251–276. Available at: https://journals-scholarsportal-info.libaccess.lib.mcmaster.ca/pdf/00664154/v47i0001/251_epopc.xml.

Cone, A.C. et al., 2013. A comparative antibody analysis of pannexin1 expression in four rat brain regions reveals varying subcellular localizations. *Front Pharmacol*, 4, p.6. Available at: http://www.ncbi.nlm.nih.gov/pubmed/23390418.

Crespo Yanguas, S. et al., 2017. Pannexin1 as mediator of inflammation and cell death. *Biochimica et Biophysica Acta - Molecular Cell Research*, 1864(1), pp.51–61.

Dahl, G., 2018. The Pannexin1 membrane channel: distinct conformations and functions. *FEBS letters*, pp.1–9. Available at: http://doi.wiley.com/10.1002/1873-3468.13115%0Ahttp://www.ncbi.nlm.nih.gov/pubmed/29802622.

DeLalio, L.J. et al., 2018. Interaction Between Pannexin 1 and Caveolin-1 in Smooth Muscle Can Regulate Blood Pressure. *Arteriosclerosis, Thrombosis, and Vascular Biology*, p.ATVBAHA.118.311290. Available at: http://atvb.ahajournals.org/lookup/doi/10.1161/ATVBAHA.118.311290.

Deneka, D. et al., 2018. Structure of a volume-regulated anion channel of the LRRC8 family. *Nature*, 558(7709), pp.254–259.

Dolmatova, E. et al., 2012. Cardiomyocyte ATP release through pannexin 1 aids in early fibroblast activation. *AJP: Heart and Circulatory Physiology*, 303(10), pp.H1208–H1218. Available at: http://ajpheart.physiology.org/cgi/doi/10.1152/ajpheart.00251.2012.

Dourado, M., Wong, E. & Hackos, D.H., 2014. Pannexin-1 is blocked by its C-terminus through a delocalized non-specific interaction surface. *PLoS ONE*, 9(6).

Draganov, D. et al., 2015. Modulation of P2X4/P2X7/Pannexin-1 sensitivity to extracellular ATP via Ivermectin induces a non-apoptotic and inflammatory form of cancer cell death. *Scientific Reports*, 5.

Dubyak, G.R. & El-Moatassim, C., 1993. Signal transduction via P2-purinergic receptors for extracellular ATP and other nucleotides. *The American journal of physiology*, 265(3 Pt 1), pp.C577-606. Available at: http://www.ncbi.nlm.nih.gov/pubmed/8214015.

Dvoriantchikova, G. et al., 2006. Expression of pannexin family of proteins in the retina. *FEBS Lett*, 580(9), pp.2178–2182. Available at: http://www.ncbi.nlm.nih.gov/entrez/query.fcgi?cmd=Retrieve&db=PubMed&dopt=Citation&list_uids=16616526.

Enkhbayar, P. et al., 2004. Structural Principles of Leucine-Rich Repeat (LRR) Proteins. *Proteins: Structure, Function and Genetics*, 54(3), pp.394–403.

Freitas-Andrade, M. & Naus, C.C., 2016. Astrocytes in neuroprotection and neurodegeneration: The role of connexin43 and pannexin1. *Neuroscience*, 323, pp.207–221. Available at: http://dx.doi.org/10.1016/j.neuroscience.2015.04.035.

Furlow, P.W. et al., 2015. Mechanosensitive pannexin-1 channels mediate microvascular metastatic cell survival. *Nature Cell Biology*, 17(7), pp.943–952.

Garre, J.M. et al., 2010. FGF-1 induces ATP release from spinal astrocytes in culture and opens pannexin and connexin hemichannels. *Proceedings of the National Academy of Sciences*, 107(52), pp.22659–22664. Available at: http://www.pnas.org/cgi/doi/10.1073/pnas.1013793107.

Gehi, R., Shao, Q. & Laird, D.W., 2011. Pathways regulating the trafficking and turnover of Pannexin1 protein and the role of the C-terminal domain. *Journal of Biological Chemistry*, 286(31), pp.27639–27653.

Gulbransen, B.D. et al., 2012. Activation of neuronal P2X7 receptor-pannexin-1 mediates death of enteric neurons during colitis. *Nature Medicine*, 18(4), pp.600–604.

Hocking, A.M., Shinomura, T. & McQuillan, D.J., 1998. Leucine-rich repeat glycoproteins of the extracellular matrix. *Matrix Biology*, 17(1), pp.1–19.

Hohenester, E., Hussain, S. & Howitt, J.A., 2006. Interaction of the guidance molecule Slit with cellular receptors. *Biochemical Society transactions*, 34(Pt 3), pp.418–21. Available at: http://biochemsoctrans.org/lookup/doi/10.1042/BST0340418%0Ahttp://www.ncbi.nlm.nih.gov/pubmed/16709176.

Huang, Y. et al., 2007. Pannexin1 is expressed by neurons and glia but does not form functional gap junctions. *Glia*, 55(1), pp.46–56.

Iglesias, R. et al., 2008. P2X7 receptor-Pannexin1 complex: pharmacology and signaling. *Am J Physiol Cell Physiol*, 295(3), pp.C752-60.

Ishikawa, M. et al., 2011. Pannexin 3 functions as an ER Ca 2+ channel, hemichannel, and gap junction to promote osteoblast differentiation. *Journal of Cell Biology*, 193(7), pp.1257–1274.

Ivanov, D. et al., 2006. Microarray analysis of gene expression in adult retinal ganglion cells. *FEBS Letters*, 580(1), pp.331–335.

Jackson, M.F., 2015. Interdependence of ATP signalling and pannexin channels; the servant was really the master all along? *Biochemical Journal*, 472(3), pp.e27–e30. Available at: http://biochemj.org/cgi/doi/10.1042/BJ20151016.

Jacobi, E. & von Engelhardt, J., 2018. AMPA receptor complex constituents: Control of receptor assembly, membrane trafficking and subcellular localization. *Molecular and Cellular Neuroscience*, 91, pp.67–75.

Jin, M.S. et al., 2007. Crystal Structure of the TLR1-TLR2 Heterodimer Induced by Binding of a Tri-Acylated Lipopeptide. *Cell*, 130(6), pp.1071–1082.

Kajava, A. V., 1998. Structural diversity of leucine-rich repeat proteins. *Journal of Molecular Biology*, 277(3), pp.519–527.

Kefauver, J.M. et al., 2018. Structure of the human volume regulated anion channel. *eLife*, 7.

Khakh, B.S. & Burnstock, G., 2009. The double life of ATP. *Scientific American*, 301(6), pp.84–92.

Kim, J.E. & Kang, T.C., 2011. The P2X7 receptor-pannexin-1 complex decreases muscarinic acetylcholine receptor-mediated seizure susceptibility in mice. *Journal of Clinical Investigation*, 121(5), pp.2037–2047.

Ko, J. & Kim, E., 2007. Leucine-rich repeat proteins of synapses. *Journal of Neuroscience Research*, 85(13), pp.2824–2832.

Kobe, B. & Deisenhofer, J., 1993. Crystal structure of porcine ribonuclease inhibitor, a protein with leucine-rich repeats. *Nature*, 366(6457), pp.751–756.

Kobe, B. & Kajava, A. V., 2001. The leucine-rich repeat as a protein recognition motif. *Current Opinion in Structural Biology*, 11(6), pp.725–732.

Koyanagi, S. et al., 2016. Glucocorticoid regulation of ATP release from spinal astrocytes underlies diurnal exacerbation of neuropathic mechanical allodynia. *Nature Communications*, 7, p.13102. Available at: http://www.nature.com/doifinder/10.1038/ncomms13102.

Kresse, H. & Schnherr, E., 2001. Proteoglycans of the extracellular matrix and growth control. *Journal of Cellular Physiology*, 189(3), pp.266–274.

Lai, C.P. et al., 2007. Tumor-suppressive effects of pannexin 1 in C6 glioma cells. *Cancer Res*,

67(4), pp.1545–1554.
Langlois, S. et al., 2014. Pannexin 1 and pannexin 3 channels regulate skeletal muscle myoblast proliferation and differentiation. *Journal of Biological Chemistry*, 289(44), pp.30717–30731.
Legouis, R. et al., 2003. Basolateral targeting by leucine-rich repeat domains in epithelial cells. *EMBO Reports*, 4(11), pp.1096–1102.
Liker, E. et al., 2000. The structure of the mRNA export factor TAP reveals a cis arrangement of a non-canonical RNP domain and an LRR domain. *EMBO Journal*, 19(21), pp.5587–98. Available at: http://www.pubmedcentral.nih.gov/articlerender.fcgi?artid=305804&tool=pmcentrez&rendertype=abstract.
Locovei, S., Bao, L. & Dahl, G., 2006. Pannexin 1 in erythrocytes: function without a gap. *Proc Natl Acad Sci U S A*, 103(20), pp.7655–7659.
Locovei, S., Wang, J. & Dahl, G., 2006. Activation of pannexin 1 channels by ATP through P2Y receptors and by cytoplasmic calcium. *FEBS Letters*, 580(1), pp.239–244.
Lohman, A.W., Billaud, M., et al., 2012. Expression of pannexin isoforms in the systemic murine arterial network. *J Vasc Res*, 49(5), pp.405–416. Available at: http://www.ncbi.nlm.nih.gov/pubmed/22739252.
Lohman, A.W. et al., 2015. Pannexin 1 channels regulate leukocyte emigration through the venous endothelium during acute inflammation. *Nature Communications*, 6, p.7965. Available at: http://www.nature.com/doifinder/10.1038/ncomms8965.
Lohman, A.W., Weaver, J.L., et al., 2012. S-nitrosylation inhibits pannexin 1 channel function. *J Biol Chem*, 287(47), pp.39602–39612. Available at: http://www.ncbi.nlm.nih.gov/pubmed/23033481.
Lohman, A.W. & Isakson, B.E., 2014. Differentiating connexin hemichannels and pannexin channels in cellular ATP release. *FEBS Lett*, 588(8), pp.1379–1388. Available at: http://www.ncbi.nlm.nih.gov/pubmed/24548565.
Ma, W. et al., 2012. Pannexin 1 forms an anion-selective channel. *Pflugers Archiv European Journal of Physiology*, 463(4), pp.585–592.
Martinon, F. & Tschopp, J., 2005. NLRs join TLRs as innate sensors of pathogens. *Trends in Immunology*, 26(8), pp.447–454.
Matilla, A. & Radrizzani, M., 2005. The Anp32 family of proteins containing leucine-rich repeats. *Cerebellum*, 4(1), pp.7–18.
Matsushima, N. et al., 2010. A nested leucine rich repeat (LRR) domain: The precursor of LRRs is a ten or eleven residue motif. *BMC Microbiology*, 10.
Matsushima, N. et al., 2007. Comparative sequence analysis of leucine-rich repeats (LRRs) within vertebrate toll-like receptors. *BMC Genomics*, 8.
Michalski, K. et al., 2018. The weak voltage dependence of pannexin 1 channels can be tuned by N-terminal modifications. *The Journal of general physiology*, pp.1–11. Available at: http://www.ncbi.nlm.nih.gov/pubmed/30377218.
Ng, A.C.Y. et al., 2011. Human leucine-rich repeat proteins: a genome-wide bioinformatic categorization and functional analysis in innate immunity. *Proceedings of the National Academy of Sciences*, 108(Supplement_1), pp.4631–4638. Available at: http://www.pnas.org/cgi/doi/10.1073/pnas.1000093107.
Ohbuchi, T. et al., 2011. Possible contribution of pannexin channel to ATP-induced currents in vitro in vasopressin neurons isolated from the rat supraoptic nucleus. *Brain Research*, 1394,

pp.71–78. Available at: http://dx.doi.org/10.1016/j.brainres.2011.04.017.
Pancer, Z. & Cooper, M., 2006. The evolution of adaptive immunity. *Immunology*, 24(1), pp.497–518.
Panchin, Y. et al., 2000. A ubiquitous family of putative gap junction molecules. *Curr Biol*, 10(13), pp.R473-4.
Pedersen, S.F., Okada, Y. & Nilius, B., 2016. Biophysics and Physiology of the Volume-Regulated Anion Channel (VRAC)/Volume-Sensitive Outwardly Rectifying Anion Channel (VSOR). *Pflugers Archiv European Journal of Physiology*, 468(3), pp.371–383.
Pelegrin, P. & Surprenant, A., 2006. Pannexin-1 mediates large pore formation and interleukin-1beta release by the ATP-gated P2X7 receptor. *EMBO J*, 25(21), pp.5071–5082. Available at: http://www.ncbi.nlm.nih.gov/entrez/query.fcgi?cmd=Retrieve&db=PubMed&dopt=Citation&list_uids=17036048.
Penuela, S. et al., 2014. Diverse post-translational modifications of the pannexin family of channel-forming proteins. *Channels*, 8(2), pp.124–130.
Penuela, S. et al., 2009. Glycosylation regulates pannexin intermixing and cellular localization. *Mol Biol Cell*, 20(20), pp.4313–4323.
Penuela, S. et al., 2012. Loss of pannexin 1 attenuates melanoma progression by reversion to a melanocytic phenotype. *J Biol Chem*, 287(34), pp.29184–29193. Available at: http://www.ncbi.nlm.nih.gov/pubmed/22753409.
Penuela, S. et al., 2007. Pannexin 1 and pannexin 3 are glycoproteins that exhibit many distinct characteristics from the connexin family of gap junction proteins. *J Cell Sci*, 120(21), pp.3772–3783. Available at: http://jcs.biologists.org/cgi/content/abstract/120/21/3772.
Penuela, S., Gehi, R. & Laird, D.W., 2013. The biochemistry and function of pannexin channels. *Biochim Biophys Acta*, 1828(1), pp.15–22. Available at: http://www.ncbi.nlm.nih.gov/pubmed/22305965.
Price, S.R., Evans, P.R. & Nagai, K., 1998. Crystal structure of the spliceosomal U2B’-U2A’ protein complex bound to a fragment of U2 small nuclear RNA. *Nature*, 394(6694), pp.645–650.
Prochnow, N. et al., 2009. Pannexin1 in the outer retina of the zebrafish, Danio rerio. *Neuroscience*, 162(4), pp.1039–1054. Available at: http://www.ncbi.nlm.nih.gov/entrez/query.fcgi?cmd=Retrieve&db=PubMed&dopt=Citation&list_uids=19409451.
Qiu, F. et al., 2011. Two non-vesicular ATP release pathways in the mouse erythrocyte membrane. *FEBS Letters*, 585(21), pp.3430–3435.
Ray, A. et al., 2005. Site-specific and developmental expression of pannexin1 in the mouse nervous system. *Eur J Neurosci*, 21(12), pp.3277–3290.
Riquelme, M.A. et al., 2013. The ATP required for potentiation of skeletal muscle contraction is released via pannexin hemichannels. *Neuropharmacology*, 75, pp.594–603.
Robinson, L.E. et al., 2014. Plasma membrane cholesterol as a regulator of human and rodent P2X7 receptor activation and sensitization. *Journal of Biological Chemistry*, 289(46), pp.31983–31994.
Rogozin, I.B. et al., 2007. Evolution and diversification of lamprey antigen receptors: Evidence for involvement of an AID-APOBEC family cytosine deaminase. *Nature Immunology*, 8(6), pp.647–656.
Sahu, G., Sukumaran, S. & Bera, A.K., 2014. Pannexins form gap junctions with

electrophysiological and pharmacological properties distinct from connexins. *Scientific Reports*, 4, pp.1–9.

Sanchez-Arias, J.C., Wicki-Stordeur, L.E. & Swayne, L.A., 2016. Perspectives on the role of pannexin 1 in neural precursor cell biology. *Neural Regeneration Research*, 11(10), pp.1540–1544.

Sanchez-Pupo, R.E., Johnston, D. & Penuela, S., 2018. N-glycosylation regulates pannexin 2 localization but is not required for interacting with pannexin 1. *International Journal of Molecular Sciences*, 19(7), pp.1–18.

Sandilos, J.K. et al., 2012. Pannexin 1, an ATP release channel, is activated by caspase cleavage of its pore-associated C terminal autoinhibitory region. *J Biol Chem*. Available at: http://www.ncbi.nlm.nih.gov/pubmed/22311983.

Santiago, M.F. et al., 2011. Targeting pannexin1 improves seizure outcome. *PLoS ONE*, 6(9), p.e25178. Available at: http://www.ncbi.nlm.nih.gov/pubmed/21949881.

Scott, P.G. et al., 2004. Crystal structure of the dimeric protein core of decorin, the archetypal small leucine-rich repeat proteoglycan. *Proceedings of the National Academy of Sciences*, 101(44), pp.15633–15638. Available at: http://www.pnas.org/cgi/doi/10.1073/pnas.0402976101.

Seminario-Vidal, L. et al., 2011. Rho signaling regulates pannexin 1-mediated ATP release from airway epithelia. *J Biol Chem*, 286(30), pp.26277–26286. Available at: http://www.ncbi.nlm.nih.gov/entrez/query.fcgi?cmd=Retrieve&db=PubMed&dopt=Citation&list_uids=21606493.

Sosinsky, G.E. et al., 2011. Pannexin channels are not gap junction hemichannels. *Channels*, 5(3), pp.193–197. Available at: http://www.ncbi.nlm.nih.gov/pubmed/21532340.

Spagnol, G., Sorgen, P.L. & Spray, D.C., 2014. Structural order in Pannexin 1 cytoplasmic domains. *Channels*, 8(2), pp.157–166.

Sridharan, M. et al., 2010. Pannexin 1 is the conduit for low oxygen tension-induced ATP release from human erythrocytes. *AJP: Heart and Circulatory Physiology*, 299(4), pp.H1146–H1152. Available at: http://ajpheart.physiology.org/cgi/doi/10.1152/ajpheart.00301.2010.

Stanley, P., 2011. Golgi glycosylation. *Cold Spring Harbor Perspectives in Biology*, 3(4), pp.1–13.

Swayne, L.A. & Bennett, S.A., 2016. Connexins and pannexins in neuronal development and adult neurogenesis. *BMC Cell Biol*, 17 Suppl 1, p.10. Available at: http://www.ncbi.nlm.nih.gov/pubmed/27230672.

Swayne, L.A., Sorbara, C.D. & Bennett, S.A., 2010. Pannexin 2 is expressed by postnatal hippocampal neural progenitors and modulates neuronal commitment. *J Biol Chem*, 285(32), pp.24977–24986.

Takahashi, N., Takahashi, Y. & Putnam, F.W., 1985. Periodicity of leucine and tandem repetition of a 24-amino acid segment in the primary structure of leucine-rich alpha 2-glycoprotein of human serum. *Proceedings of the National Academy of Sciences*, 82(7), pp.1906–1910. Available at: http://www.pnas.org/cgi/doi/10.1073/pnas.82.7.1906.

Thompson, R.J. et al., 2008. Activation of pannexin-1 hemichannels augments aberrant bursting in the hippocampus. *Science*, 322(5907), pp.1555–1559.

Thompson, R.J., Zhou, N. & MacVicar, B.A., 2006. Ischemia Opens Neuronal Gap Junction Hemichannels. *Science*, 312(5775), pp.924–927. Available at: http://www.sciencemag.org/cgi/content/abstract/312/5775/924.

Turmel, P. et al., 2011. Characterization of pannexin1 and pannexin3 and their regulation by

androgens in the male reproductive tract of the adult rat. *Molecular Reproduction and Development*, 78(2), pp.124–138.

Le Vasseur, M. et al., 2014. Pannexin 2 protein expression is not restricted to the CNS. *Frontiers in cellular neuroscience*, 8(392), pp.1–13.

Vogt, A., Hormuzdi, S.G. & Monyer, H., 2005. Pannexin1 and Pannexin2 expression in the developing and mature rat brain. *Brain Res Mol Brain Res*, 141(1), pp.113–120.

Vroman, R. et al., 2014. Extracellular ATP Hydrolysis Inhibits Synaptic Transmission by Increasing pH Buffering in the Synaptic Cleft. *PLoS Biology*, 12(5).

Wang, J. et al., 2014. The membrane protein Pannexin1 forms two open-channel conformations depending on the mode of activation. *Science Signaling*, 7(335), p.ra69-ra69. Available at: http://stke.sciencemag.org/cgi/doi/10.1126/scisignal.2005431.

Wang, J. & Dahl, G., 2018. Pannexin1: a multifunction and multiconductance and/or permeability membrane channel. *American Journal of Physiology-Cell Physiology*, 315(3), pp.C290–C299. Available at: https://www.physiology.org/doi/10.1152/ajpcell.00302.2017.

Wang, J. & Dahl, G., 2010. SCAM analysis of Panx1 suggests a peculiar pore structure. *The Journal of general physiology*, 136, pp.515–527.

Wang, J., Jackson, D.G. & Dahl, G., 2018. Cationic control of Panx1 channel function. *American Journal of Physiology-Cell Physiology*, 315(3), pp.C279–C289. Available at: https://www.physiology.org/doi/10.1152/ajpcell.00303.2017.

Wang, X.H. et al., 2009. Identification and characterization of pannexin expression in the mammalian cochlea. *J Comp Neurol*, 512(3), pp.336–346.

Weilinger, N.L. et al., 2016. Metabotropic NMDA receptor signaling couples Src family kinases to pannexin-1 during excitotoxicity. *Nat Neurosci*, 19(3), pp.432–442. Available at: http://www.ncbi.nlm.nih.gov/pubmed/26854804.

Weilinger, N.L., Tang, P.L. & Thompson, R.J., 2012. Anoxia-induced NMDA receptor activation opens pannexin channels via Src family kinases. *J Neurosci*, 32(36), pp.12579–12588. Available at: http://www.ncbi.nlm.nih.gov/pubmed/22956847.

West, A.P., Koblansky, A.A. & Ghosh, S., 2006. Recognition and Signaling by Toll-Like Receptors. *Annual Review of Cell and Developmental Biology*, 22(1), pp.409–437. Available at: http://www.annualreviews.org/doi/10.1146/annurev.cellbio.21.122303.115827.

Wicki-Stordeur, L.E. et al., 2016. Pannexin 1 Differentially Affects Neural Precursor Cell Maintenance in the Ventricular Zone and Peri-Infarct Cortex. *Journal of Neuroscience*, 36(4), pp.1203–1210.

Wicki-Stordeur, L.E. et al., 2012. Pannexin 1 regulates postnatal neural stem and progenitor cell proliferation. *Neural development*, 7(1), p.11. Available at: http://www.ncbi.nlm.nih.gov/pubmed/22458943.

Wicki-Stordeur, L.E., Boyce, A.K. & Swayne, L.A., 2013. Analysis of a pannexin 2-pannexin 1 chimeric protein supports divergent roles for pannexin C-termini in cellular localization. *Cell communication & adhesion*, 20(3–4), pp.73–79. Available at: http://www.ncbi.nlm.nih.gov/pubmed/23659289.

Wicki-Stordeur, L.E. & Swayne, L.A., 2013. Panx1 regulates neural stem and progenitor cell behaviours associated with cytoskeletal dynamics and interacts with multiple cytoskeletal elements. *Cell Communication and Signaling*, 11(1).

de Wit, J. et al., 2011. Role of Leucine-Rich Repeat Proteins in the Development and Function of Neural Circuits. *Annual Review of Cell and Developmental Biology*, 27(1), pp.697–729.

Available at: http://www.annualreviews.org/doi/10.1146/annurev-cellbio-092910-154111.
Zhang, Y. et al., 2015. Pannexin-1 up-regulation in the dorsal root ganglion contributes to neuropathic pain development. *Journal of Biological Chemistry*, 290(23), pp.14647–14655.